

Figure 2 Pluripotency of AM and YS-miPSCs. (a) Chimeric mice with female AM-miPSCs and male YS-miPSCs. Inset: X-gal staining of testis collected from an adult YS-miPSC chimera (blue cells are YS-miPSC derivatives). (b) Immunohistochemical double staining of testis cryosections from a YS-miPSC chimera with anti-LacZ (YS-miPSC-derived germ cells) and anti-TRA98 (spermatogonia and spermatocytes) antibodies. (c) Genotyping of progeny obtained by backcrossing with YS-miPSC chimeras. *Neo* positive demonstrates germline transmission of YS-miPSC genetic information. *Gapdh* is positive control. (d) Hematoxylin-eosin staining of teratoma sections generated by AM and YS-miPSC implantation. GL, glia (ectoderm); NE, neuroepithelium (ectoderm); CE, ciliated epithelium (endoderm); CA, cartilage (ectoderm); MU, muscle (mesoderm). (e) Transcription analysis of lineage-specific genes in teratomas generated with AM and YS-miPSCs. Gray rectangle: endoderm makers; purple rectangle: mesoderm markers; pink rectangle: ectoderm markers. *Afp*, α -Fetoprotein; *Alb*, albumin; *Des*, desmin; *Nes*, Nestin; *Nf-m*, neurofilament-M; *Gdh*, *Gapdh* (positive control).

of key pluripotency genes was examined by bisulfite-modified DNA sequencing. Promoters of both *OCT4* and *NANOG* were found to highly methylated in hAM cells, consistent with transcriptional silencing in these cells. Conversely, both promoter regions were hypo-methylated in AM-hiPSCs consistent with the observed reactivation (Fig. 3d). These data demonstrate that human AM cells are capable of being epigenetically reprogrammed to AM-hiPSCs through forced expression of reprogramming factors.

Teratoma formation with AM-hiPSCs

To address whether the AM-hiPSCs have competence to differentiate into specific tissues, teratoma formation was induced by implantation under the kidney capsule of immunodeficient nude mice. Twenty-one out of twenty-four AM-hiPSC independent clones induced teratoma formation within 6–10 weeks of implantation (1.0×10^7 cells/site). Histological analysis by HE staining of paraffin-embedded sections demonstrated that the three

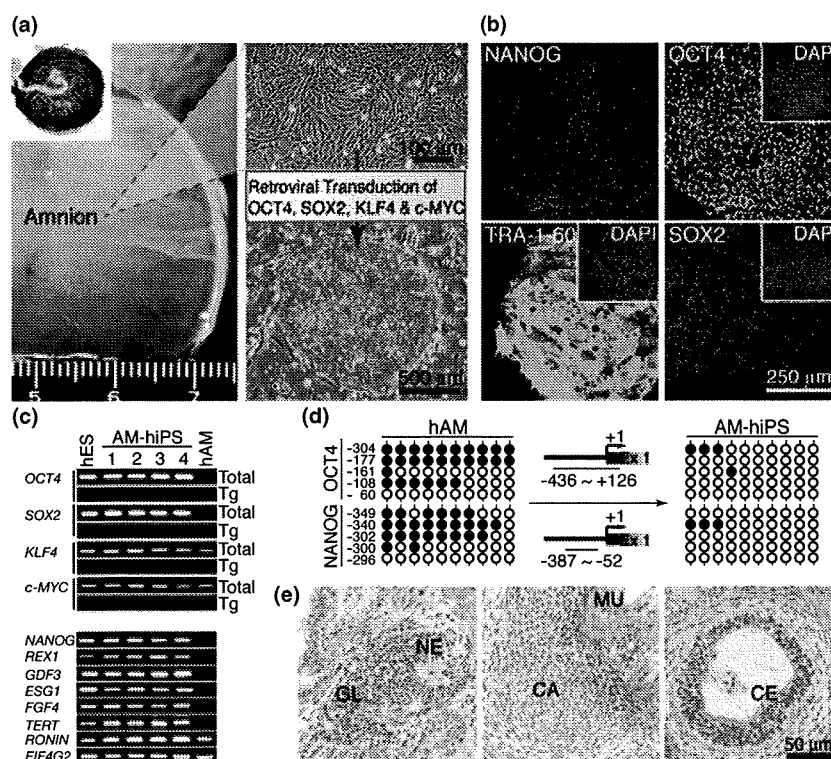


Figure 3 Generation of iPSCs from human AM cells. (a) Isolation of hAM cells from extra-embryonic tissues of human newborns and generation of hiPSCs through epigenetic reprogramming by retroviral infection-mediated expression of *OCT4*, *SOX2*, *KLF4* and *c-MYC*. (b) Expression of pluripotent cell marker proteins, NANOG, OCT4, TRA-1-60 and SOX2. Cell nuclei were visualized with DAPI. (c) Transcriptional activation of pluripotent marker genes by hiPSC induction. RT-PCR analyses revealed that the exogenous *OCT4*, *SOX2*, *KLF4* and *c-MYC* genes were silenced and the endogenous pluripotent marker genes were activated in AM-hiPSCs. *KLF4*, *c-MYC* and *RONIN* were expressed even in hAM cells before reprogramming. *EIF4G2* (*eukaryotic translation initiation factor 4 gamma 2*) is included as a positive control. (d) Epigenetic reprogramming of the *OCT4* and *NANOG* promoter regions. Bisulfite-modified DNA sequence analysis demonstrated a transition from hyper-methylation in AM cells (black circles) to hypo-methylation in AM-hiPSCs (white circles). (e) Hematoxylin-eosin staining of teratoma sections of teratoma generated by AM-hiPSC implantation. GL, glia (ectoderm); NE, neuroepithelium (ectoderm); CE, ciliated epithelium (endoderm); CA, cartilage (ectoderm); MU, muscle (mesoderm).

primary layers were generated as shown by ectodermal glia and neuroepithelium, mesodermal muscle and endodermal ciliated epithelium and cartilage morphologically (Fig. 3e). Thus, the majority of AM-hiPSC clones have potential for multi-lineage differentiation *in vivo*.

Discussion

We here demonstrated that hiPSCs and miPSCs were efficiently generated from newborn AM cells, in which endogenous *Klf4*, *c-Myc* and *Ronin* were highly expressed. The generation efficiency of miPSCs from AM cells was comparable to that from MEFs in mice and was notably high to that from adult somatic cells in humans. The properties of AM-hiPSCs and AM or

YS-miPSCs resemble those of fully reprogrammed iPSCs from other tissues and ESCs.

iPSCs are generated through epigenetic reprogramming of somatic cells. Information on the base sequence of DNA in nuclei is unchanged through the reprogramming, although the gene expression profile is altered through the reprogramming from the somatic cell to the iPSC type. Developmentally rewound iPSCs retain aged DNA base sequence information inherited from somatic cells. The base sequence of DNA accumulates mutations through aging with cell division and mis-repair. Young somatic cells are suitable for iPSC generation rather than aged somatic cells. Therefore, it is suggested that the AM cells accumulating less genetic mutation are safer than the adult somatic cells as a cell source for iPSC generation.

The generation efficiency of OG-positive colonies was approximately four times lower than that of ALP-positive colonies and it is likely that miPSC generation will be further reduced (Wernig *et al.* 2008). Furthermore, when pre-iPSCs are reseeded, the generation efficiency of iPSC outcome could be roughly estimated as $1/2^X$ (X = reseeded day after infection or transfection; doubling time of pre-iPSC is estimated as 24 h). Recently, iPSC generation technology has been developed and improved with MEFs and human embryonic or newborn fibroblasts (HNFs) as representative somatic cells. Even with these types of cells, application of the current technology resulted in a marked decrease in iPSC generation efficiency. The retroviral transduction-mediated miPSC generation efficiency is 0.05–0.1% with MEFs (Takahashi *et al.* 2007; Wernig *et al.* 2007). The generation efficiency of hiPSCs ($\sim 0.01\%$ in ALP-positive colony and 0.0025% in hiPSC outcome) (Yu *et al.* 2007; Wernig *et al.* 2008) is ~ 10 times lower than that of miPSCs. The generation efficiency of genetic modification-free hiPSCs from HNFs by direct delivery of reprogramming proteins is estimated at about 0.001% in outcome (Kim *et al.* 2009). Notably, it is evident that the generation of hiPSCs from adult somatic cells is much harder than that from MEFs. In fact, analysis with a secondary dox-inducible transgene system shows that the efficiency varies between different somatic cell types (Wernig *et al.* 2008). Thus, for practical application of iPSC technology to medical care, identification of reprogramming-sensitive cell types is a key issue. Human primary keratinocytes are one candidate cell type for efficient generation of hiPSCs from adult patients (the efficiency of ALP-positive colony = 1.0%) (Aasen *et al.* 2008). Here, we have shown that human and mouse AM cells, in which the endogenous *KLF4/Klf4*, *c-MYC/c-Myc* and *RONIN/Ronin* are naturally expressed, are highly reprogramming-sensitive (hiPSC generation efficiency was approximately 0.02% in outcome). An important point is that relatively huge amounts of human AM cells can be collected from discarded AM membranes at birth with no risk to the individual. Furthermore, these cells can be kept in long-term storage without requirement for amplification by in vitro cell culture.

Our findings illustrate that human AM cells are a strong candidate cell source for collection and banking that could be retrieved on demand and used for generating personalized genetic modification-free iPSCs applicable for clinical treatment and drug screening.

Experimental procedures

Amnion and yolk sac cells

In mice, AM and YS membranes collected from E18.5 embryos from GOF-18/delta PE/GFP (Oct4-GFP) transgenic females (Yoshimizu *et al.* 1999) mated with 129/Rosa26 transgenic males (Friedrich & Soriano 1991) were digested with 0.1% collagenase (Wako, Osaka, Japan) and 20% fetal bovine serum (FBS) at 37 °C for 1 h, and then repeatedly passed through a 26-gauge needle. The cell suspension was cultured with mES medium (DMEM/F12 (Dulbecco's modified Eagle's medium/Ham's F12) (Wako) supplemented with 15% FBS, 10^{-4} M 2-mercaptoethanol (Sigma) and 1000 U/mL of recombinant leukemia inhibitory factor (Chemicon, Temecula, CA, USA) containing 5 ng/mL basic fibroblast growth factor (bFGF) (Peprotech, Rocky Hill, NJ, USA). Following culture for 2–3 days, the adherent AM and YS cells growing to near-confluence were applied for iPSC experiments.

In humans, the AM membrane was cut into tiny pieces with dissection scissors. The AM membrane pieces were cultured in DMEM with 10% FBS for 7–10 days. The adherent AM cells growing to near-confluence were applied for iPSC experiments. Primary AM cells were provided from the cell bank of RIKEN Bioresource Center, Japan.

Generation of iPSCs

In mouse, each of pMXs-Oct4, Sox2, Klf4, c-Myc and DsRed (an indicator of retroviral silencing) was transfected into the Plat-E cells using the FuGENE6 Transfection Reagent (Roche Diagnostics, Indianapolis, IN, USA). A 1 : 1 : 1 : 1 : 4 mixture of Oct4, Sox2, Klf4, c-Myc and DsRed retroviruses in supernatants with 4 μ g/mL polybrene (Nacalai Tesque, Kyoto, Japan) was added to AM and YS cells at 1.0×10^5 cells per 3 cm well. At day 4 after infection, the cells were reseeded into a 10 cm culture dish on feeder cells with mES medium. Colonies were picked around day 20.

In humans, pMXs-OCT4, SOX2, KLF4 or c-MYC, pCL-GagPol, and pHCMV-VSV-G vectors were transfected into 293FT cells (Invitrogen, Carlsbad, CA, USA) using the TransIT-293 reagent (Mirus). A 1 : 1 : 1 : 1 mixture of OCT4, SOX2, KLF4 and c-MYC viruses in supernatant with 4 μ g/mL polybrene were added to AM cells at 1.0×10^5 cells per 3 cm well. The cells were subcultured on feeder cells into a 10 cm dish with the iPSellon medium (Cardio) supplemented with 10 ng/mL bFGF (Wako) (hES medium). Colonies were picked up around day 28.

Immunocytochemistry

Human and mouse cells were fixed with 4% paraformaldehyde in phosphate-buffered saline (PBS) for 10 min at 4 °C. After washing with 0.1% Triton X-100 in PBS (PBST), the cells were prehybridized with blocking buffer for 1–12 h at 4 °C and then incubated with primary antibodies; anti-SSEA4

Table 1 Primers for RT-PCR and PCR

Gene name	5'-Forward-3'	5'-Reverse-3'
Mice		
<i>Oct4</i> (total)	CTGAGGGCCAGGCAGGAGCACGAG	CTGTAGGGAGGGCTTCGGGCACTT
<i>Oct4</i> (endogenous)	TCTTTCCACCAGGCCCCCGGCTC	TGCGGGCGGACATGGGGAGATCC
<i>Oct4</i> (transgene)	CCCATGGTGGTGGTACGGGAATTC	AGTTGCTTTCCACTCGTGCT
<i>Sox2</i> (total)	GGTTACCTCTTCTCCACTCCAG	TCACATGTGCGACAGGGGCAG
<i>Sox2</i> (transgene)	CCCATGGTGGTGGTACGGGAATTC	TCTCGGTCTCGGACAAAAGT
<i>Klf4</i> (total)	CACCATGGACCCGGGCGTGGCTGCCAGAAA	TTAGGCTGTTCTTTTCCGGGGCCACGA
<i>Klf4</i> (endogenous)	GCGAACTCACACAGGCGAGAAACC	TGCTTCTCTTCTCCTCCGACACA
<i>Klf4</i> (transgene)	CCCATGGTGGTGGTACGGGAATTC	GTCGTTGAACTCCTCGGTCT
<i>c-Myc</i> (total)	CAGAGGAGGAACGAGCTGAAGCGC	TTATGCACCAGAGTTTGAAGCTGTTCG
<i>c-Myc</i> (endogenous)	CAGAGGAGGAACGAGCTGAAGCGC	AAGTTTGAGGCAGTTAAAATTATGGCTGAAGC
<i>c-Myc</i> (transgene)	CTCCTGGCAAAAAGGTCAGAG	GACATGGCCTGCCCGGTTATTATT
<i>Nanog</i>	ATGAAGTGCAAGCGGTGGCAGAAA	CCTGGTGGAGTCACAGAGTAGTTC
<i>Eras</i>	CAAAGATGCTGGCAGGCAGCTACC	GACAAGCAGGGCAAAGGCTTCCTC
<i>Gdf3</i>	AGTTTCTGGGATTAGAGAAAAGC	GGGCCATGGTCAACTTTGCCT
<i>Rex1</i>	GACATCATGAATGAACAAAAAATG	CCTTCAGCATTTCTTCCCTG
<i>Zfp296</i>	AAGCACCCAGATCTGTTGACCT	GAGCCTCTGGGGTATCTAGG
<i>Ronin</i>	GCCTCAGAGCTAGAGGCTGCTACG	TGGAAGGAGTCACGAATTCTGCAG
<i>Igf1</i>	GGACCAGAGACCCCTTGCGGGG	GGCTGCTTTTGTAGGCTTCAGTGG
<i>Cd6</i>	CCTAAGCACCCCTGAAGCAAG	ACAACCTGGGAACCCACAAAAGC
<i>Gapdh</i>	CCCACTAACATCAAATGGGG	CCTTCCACAATGCCAAAAGT
α - <i>Fetoprotein</i>	TCGTATTCCAACAGGAGG	CACTCTTCTTCTGGAGATG
<i>Albumin</i>	AAGGAGTGCTGCCATGGTGA	CCTAGGTTTCTTGCAACCTC
<i>Myf-5</i>	TGCCATCCGCTACATTGAGAG	CCGGGTAGCAGGCTGTGAGTTG
<i>MyoD</i>	GCCCCGCGCTCCAACTGCTCTGAT	CCTACGGTGGTGCGCCCTCTGC
<i>Desmin</i>	TTGGGGTCGCTGCGGTCTAGCC	GGTCGTCTATCAGGTTGTACG
<i>Nestin</i>	GGAGTGTCGCTTAGAGGTGC	TCCAGAAAAGCCAAGAGAAGC
<i>Neurofilament-M</i>	GCCGAGCAGACCAAGGAGGCCATT	CTGGATGGTGTCTCTGGTAGCTGCT
<i>Neo</i>	CGGCAGGAGCAAGGTGAGAT	CAAGATGGATTGCACGCAGG
Humans		
<i>OCT4</i> (total)	GCCGTATGAGTTCTGTGG	TCTCCTTCTCCAGCTTAC
<i>SOX2</i> (total)	TAAGTACTGGCGAACCATCT	AAATTACCAACGGTGTCAAC
<i>KLF4</i> (total)	ACTCGCCTTGCTGATTGTCT	GAACGTGGAGAAAGATGGGA
<i>c-MYC</i> (total)	GCGTCTGGGAAGGGAGATCCGGAGC	TTGAGGGGCATCGTCGCGGGAGGCTG
<i>NANOG</i>	ATTATGCAGGCAACTCACTT	GATTCTTTACAGTCGGATGC
<i>REX1</i>	CAGATCCTAAACAGCTCGCAGAAT	GCGTACGCAAATTAAGTCCAGA
<i>GDF3</i>	CTTATGCTACGTAAAGGAGCGGG	GTGCCAACCCAGGTCCCAGGAGTT
<i>ESG1</i>	ATATCCC GCCGTGGGTGAAAGTTT	ACTCAGCCATGGACTGGAGCATCC
<i>FGF4</i>	CTACAACGCCCTACGAGTCCCTACA	GTTGCACCAGAAAAGTCAGAGTTG
<i>TERT</i>	CCTGCTCAAGCTGACTCGACACCGTG	GGAAAAGCTGGCCCTGGGGTGGAGC
<i>RONIN</i>	CACTGTAGACAGCAGTCAGG	TGCCCTTTCATCTCTTTCATC
<i>EIF4G2</i>	AAGGAAAGGGACTGAGTTTC	CCAAGAAAAGCTTCTTCTTCA
<i>Bis-OCT4</i>	GATTAGTTTGGGTAATATAGTAAGGT	ATCCCACCCACTAACCTTAACCTCTA
<i>Bis-NANOG</i>	TGGTTAGGTTGGTTTTAAATTTTTG	AACCCACCCTTATAAATTCTCAATTA

(1 : 300) (Chemicon), anti-TRA-1-60 (1 : 300) (Chemicon), anti-Oct4 (1 : 50) (Santa Cruz Biotechnology, Santa Cruz, CA, USA), anti-Nanog (1 : 300) (ReproCELL, Tokyo, Japan), anti-Sox2 (1 : 300) (Abcam, Cambridge, UK) and/or anti-SSEA1 (1 : 1000) (DSHB) antibodies for 6–12 h at 4 °C. They were incubated with secondary antibodies; anti-rabbit

IgG, anti-mouse IgG or anti-mouse IgM conjugated with Alexa 488 or 546 (1 : 500) (Molecular Probes, Eugene, OR, USA) in blocking buffer for 1 h at room temperature. The cells were counterstained with 4,6-diamidino-2-phenylindole (DAPI) and then mounted with a SlowFade light antifade kit (Molecular Probes). To examine germline competence,

cryosections of a half of a testis of 4- to 5-week-old chimeric mice were fixed with 4% paraformaldehyde in PBS for overnight at 4 °C, and then prehybridized with blocking buffer. The sections were double-stained with primary antibodies; anti-LacZ antibody (1 : 500) (Promega, Madison, WI, USA) specific to miPSC-derived cells and with anti-TRA98 antibody (1 : 500) specific to spermatogonia and spermatocytes. The remaining testis and ovaries were stained with X-gal.

RT-PCR

Total RNAs were isolated from mouse and human cells using the TRIzol (Invitrogen) and the RNeasy Plus Mini Kit (Qiagen, Valencia, CA, USA), respectively. cDNAs were synthesized from 1 µg total RNAs using Superscript III reverse transcriptase (Invitrogen) with random hexamers according to the manufacturer's instructions. Template cDNA was PCR-amplified with gene-specific primer sets (Table 1).

Gene expression microarray

Total RNA was extracted from mouse cells using the TRIzol Reagent. Double-stranded cDNA synthesized from the total RNA was amplified and labeled using the One-Cycle Target Labeling and Control Regents (Affymetrix, Santa Clara, CA, USA). Global gene expression was examined with the GeneChip Mouse Genome 430 2.0 Array (Affymetrix). The fluorescence intensity of each probe was quantified by using the GeneChip Analysis Suite 5.0 computer program (Affymetrix). The level of gene expression was determined as the average difference (AD). Specific AD levels were then calculated as percentages of the mean AD level of probe sets for housekeeping genes *Actin* and *Gapdh*. To eliminate changes within the range of background noise and to select the most differentially expressed genes, data were used only if the raw data values were less than 50 AD. Further data were analyzed with GeneSpring GX 7.3.1 (Agilent Technologies, Santa Clara, CA, USA).

Reprogramming efficiency

The reprogramming efficiency of mouse YS and AM cells was estimated by counting the number of ALP-positive colonies 21 days after retroviral infection. The cells in 10 cm culture dish were fixed with 4% paraformaldehyde in PBS for 15 min at room temperature and washed with PBS. After treating with ALP stain (pH 9.0) for 30 min at room temperature, the number of ALP-positive cells was counted.

Chimera

AM-miPSCs ($2n = 40$, XX) and YS-miPSCs ($2n = 40$, XY) were microinjected into blastocysts (C57BL/6j × BDF1). The blastocysts were transferred into the uterus of pseudopregnant ICR female mice. Chimeric mice were mated with C57BL/6j

for examining germline transmission. The genotype of the progeny was determined with tail tip DNA by genomic PCR with a *Neo*-specific primer set (Table 1). All animal experiments were performed according to the guidelines of animal experiments of Kyoto University, Japan.

Teratoma

In mice, cell suspension of 1.0×10^6 AM or YS-miPSCs/100 µL DMEM/F12 was subcutaneously injected into the inguinal region of immunodeficient SCID mice (CLEA). In humans, the 1 : 1 mixture of the AM-hiPSC suspension and Basement Membrane Matrix (BD Biosciences, San Jose, CA, USA) were implanted at 1.0×10^7 cells/site under the kidney capsule of immunodeficient nude mice (CLEA). Teratomas surgically dissected out 5–8 weeks in mice and 6–10 weeks in human after implantation, were fixed with 4% paraformaldehyde in PBS, and embedded in paraffin. Sections at 10 µm in thickness were stained with HE.

Bisulfite-modified DNA sequencing

Genomic DNAs (1 µg) extracted from AM-hiPSCs and hAM cells were bisulfite-treated with EZ DNA methylation-Gold Kit (ZYMO Research, Orange, CA, USA) according to the manufacturer's instruction. The promoter regions of the human *NANOG* and *OCT4* genes were PCR-amplified with specific primer sets (Table 1). Ten clones of each PCR product were gel-purified, sub-cloned and sequenced with the SP6 universal primer.

Acknowledgements

We thank Dr Gen Kondoh and Miss Hitomi Watanabe for generating chimeras, and Dr Justin Ainscough for critical comments on the manuscript.

References

- Aasen, T., Raya, A., Barrero, M.J., Garreta, E., Consiglio, A., Gonzalez, F., Vassena, R., Bilic, J., Pekarik, V., Tiscornia, G., Edel, M., Boue, S. & Belmonte, J.C. (2008). Efficient and rapid generation of induced pluripotent stem cells from human keratinocytes. *Nat. Biotechnol.* **26**, 1276–1284.
- Brambrink, T., Foreman, R., Welstead, G.G., Lengner, C.J., Wernig, M., Suh, H. & Jaenisch, R. (2008). Sequential expression of pluripotency markers during direct reprogramming of mouse somatic cells. *Cell Stem Cell* **2**, 151–159.
- Curran, T., Miller, A.D., Zokas, L. & Verma, I.M. (1984). Viral and cellular fos proteins: a comparative analysis. *Cell* **36**, 259–268.
- Feng, B., Ng, J.H., Heng, J.C. & Ng, H.H. (2009). Molecules that promote or enhance reprogramming of somatic cells to induced pluripotent stem cells. *Cell Stem Cell* **4**, 301–312.

Friedrich, G. & Soriano, P. (1991). Promoter traps in embryonic stem cells: a genetic screen to identify and mutate developmental genes in mice. *Genes Dev.* **5**, 1513–1523.

Jaenisch, R. & Young, R. (2008). Stem cells, the molecular circuitry of pluripotency and nuclear reprogramming. *Cell* **132**, 567–582.

Kim, D., Kim, C.H., Moon, J.I., Chung, Y.G., Chang, M.Y., Han, B.S., Ko, S., Yang, E., Cha, K.Y., Lanza, R. & Kim, K.S. (2009). Generation of human induced pluripotent stem cells by direct delivery of reprogramming proteins. *Cell Stem Cell* **4**, 472–476.

Nakagawa, M., Koyanagi, M., Tanabe, K., Takahashi, K., Ichisaka, T., Aoi, T., Okita, K., Mochiduki, Y., Takizawa, N. & Yamanaka, S. (2008). Generation of induced pluripotent stem cells without Myc from mouse and human fibroblasts. *Nat. Biotechnol.* **26**, 101–106.

Sridharan, R. & Plath, K. (2008). Illuminating the black box of reprogramming. *Cell Stem Cell* **2**, 295–297.

Takahashi, K., Okita, K., Nakagawa, M. & Yamanaka, S. (2007). Induction of pluripotent stem cells from fibroblast cultures. *Nat. Protoc.* **2**, 3081–3089.

Wernig, M., Lengner, C.J., Hanna, J., Lodato, M.A., Steine, E., Foreman, R., Staerk, J., Markoulaki, S. & Jaenisch, R. (2008). A drug-inducible transgenic system for direct reprogramming of multiple somatic cell types. *Nat. Biotechnol.* **26**, 916–924.

Wernig, M., Meissner, A., Foreman, R., Brambrink, T., Ku, M., Hochedlinger, K., Bernstein, B.E. & Jaenisch, R. (2007). In vitro reprogramming of fibroblasts into a pluripotent ES-cell-like state. *Nature* **448**, 318–324.

Yamanaka, S. (2007). Strategies and new developments in the generation of patient-specific pluripotent stem cells. *Cell Stem Cell* **1**, 39–49.

Yoshimizu, T., Sugiyama, N., De Felice, M., Yeom, Y.I., Ohbo, K., Masuko, K., Obinata, M., Abe, K., Scholer, H.R. & Matsui, Y. (1999). Germline-specific expression of the Oct-4/green fluorescent protein (GFP) transgene in mice. *Dev. Growth Differ.* **41**, 675–684.

Yu, J., Vodyanik, M.A., Smuga-Otto, K., Antosiewicz-Bourget, J., Frane, J.L., Tian, S., Nie, J., Jonsdottir, G.A., Ruotti, V., Stewart, R., Slukvin, I.I. & Thomson, J.A. (2007). Induced pluripotent stem cell lines derived from human somatic cells. *Science* **318**, 1917–1920.

Zhou, H., Wu, S., Joo, J.Y., Zhu, S., Han, D.W., Lin, T., Trauger, S., Bien, G., Yao, S., Zhu, Y., Siuzdak, G., Scholer, H.R., Duan, L. & Ding, S. (2009). Generation of induced pluripotent stem cells using recombinant proteins. *Cell Stem Cell* **4**, 381–384.

Received: 20 August 2009

Accepted: 16 September 2009

羊膜から効率よく iPS細胞

胎児を含む羊膜を使って効率よくiPS(人工多能性幹)細胞をつくることに、京都大再生医学研究所の多田高准教授らが成功し、16日に専門誌に発表した。ヒトでもマウスでも確認された。羊膜は長く保存できるため、将来構想されるiPS細胞バンクで使用する細胞の候補になる可能性がある。同研究所の山中伸弥教授や国立成育医療センター研究所との共同研究。

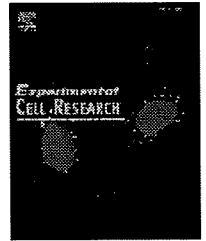
京都大などのグループ発表

iPS細胞は、体細胞に四つの遺伝子を入れてつくる。多田准教授らは、羊膜の細胞では2遺伝子がすでに働いていることに注目した。羊膜の細胞に4遺伝子を組み込んでiPS細胞をつくったところ、大人の体の細胞からつくるより、iPS細胞ができる率は10倍以上となり、効率よくできた。

iPS細胞の作製効率を高める方法としては、特定の遺伝子の働きを抑えたり、化学物質を使ったりするなどの報告があるが、羊膜からつくる方法はより操作が少なくて済むという。多田准教授は「出産時に胎盤とともに出てくる羊膜を保存し、必要になったときにiPS細胞をつくるような応用が考えられる」と話している。(瀬川茂子)



101種類のヒトiPS作製(図5) を発表した論文



Research Article

Mesenchymal to embryonic incomplete transition of human cells by chimeric OCT4/3 (POU5F1) with physiological co-activator EWS

Hatsune Makino^a, Masashi Toyoda^a, Kenji Matsumoto^b, Hirohisa Saito^b, Koichiro Nishino^a, Yoshihiro Fukawatase^a, Masakazu Machida^a, Hidenori Akutsu^a, Taro Uyama^a, Yoshitaka Miyagawa^c, Hajime Okita^c, Nobutaka Kiyokawa^c, Takashi Fujino^{d,f}, Yuichi Ishikawa^e, Takuro Nakamura^d, Akihiro Umezawa^{a,*}

^a Department of Reproductive Biology, National Institute for Child Health and Development, Tokyo, 157-8535, Japan

^b Department of Allergy and Immunology, National Institute for Child Health and Development, Tokyo, 157-8535, Japan

^c Department of Developmental Biology and Pathology, National Institute for Child Health and Development, Tokyo, 157-8535, Japan

^d Department of Carcinogenesis, The Cancer Institute, Japanese Foundation for Cancer Research, Tokyo, 140-8455, Japan

^e Department of Pathology, The Cancer Institute, Japanese Foundation for Cancer Research, Tokyo, 140-8455, Japan

^f Department of Pathology, Faculty of Medicine, Kyorin University, Tokyo, 181-8611, Japan

ARTICLE INFORMATION

Article Chronology:

Received 7 November 2008

Revised version received 15 June 2009

Accepted 16 June 2009

Available online 24 June 2009

Keywords:

Dedifferentiation

Mesoderm

Embryonic carcinoma

iPS cell

OCT4/3

Stem cell

ABSTRACT

POU5F1 (more commonly known as OCT4/3) is one of the stem cell markers, and affects direction of differentiation in embryonic stem cells. To investigate whether cells of mesenchymal origin acquire embryonic phenotypes, we generated human cells of mesodermal origin with overexpression of the chimeric OCT4/3 gene with physiological co-activator EWS (product of the *EWSR1* gene), which is driven by the potent EWS promoter by translocation. The cells expressed embryonic stem cell genes such as *NANOG*, lost mesenchymal phenotypes, and exhibited embryonic stem cell-like alveolar structures when implanted into the subcutaneous tissue of immunodeficient mice. Hierarchical analysis by microchip analysis and cell surface analysis revealed that the cells are subcategorized into the group of human embryonic stem cells and embryonic carcinoma cells. These results imply that cells of mesenchymal origin can be traced back to cells of embryonic phenotype by the OCT4/3 gene in collaboration with the potent cis-regulatory element and the fused co-activator. The cells generated in this study with overexpression of chimeric OCT4/3 provide us with insight into cell plasticity involving OCT4/3 that is essential for embryonic cell maintenance, and the complexity required for changing cellular identity.

© 2009 Elsevier Inc. All rights reserved.

Introduction

Somatic stem cells have been shown to have a more flexible potential, but the conversion of mesenchymal cells to embryonic stem (ES) cells has still been a challenge and requires gene transduction

[1–4]. This phenotypic conversion requires the molecular reprogramming of mesenchyme. Mesenchymal stem cells or mesenchymal progenitors have been isolated from adult bone marrow [5], adipose tissue [6], dermis [7], endometrium [8], menstrual blood [8], cord blood [9,10], and other connective tissues [11]. These cells are

* Corresponding author. Fax: +81 3 5494 7048.

E-mail address: umezawa@1985.jkuin.keio.ac.jp (A. Umezawa).

capable of differentiating into osteoblasts [12], chondrocytes [13], skeletal myocytes, adipocytes, cardiomyocytes [14,15], and neural cells [16]. However, most of the differentiation capability is limited to cells of mesodermal origin. This is in contrast to ES cells derived from the inner cell mass of the blastocyst that differentiate into cells of three germ cell layers. ES cells are pluripotent and immortal, and, therefore, ES cells provide an unlimited number of specialized cells.

Embryonic and adult fibroblasts have been induced to become pluripotent stem cells (iPS cells) or ES-like cells by defined factors including POU5F1 (also known as OCT4/3) [1–3]. OCT4/3 protein, a member of the POU family of transcription factors, is related to the pluripotent capacity of ES cells, and is thus a distinctive marker to identify primordial germ and embryonic stem cells [17–21]. OCT4/3 is down-regulated during oogenesis and spermatogenesis [22]. Furthermore, knocking out the OCT4/3 gene in mice causes early lethality because of lack of inner cell mass formation [23], and OCT4/3 is critical for self-renewal of ES cells [24]. During human development, expression of OCT4/3 is found at least until the blastocyst stage [25] in which it is involved in gene expression regulation. OCT4/3 functions as a master switch in differentiation by regulating cells that have, or can develop, pluripotent potential by activating transcription via octamer motifs [26].

The EWS gene was originally identified at the chromosomal translocation, and fused with the ets transcription factors in Ewing sarcoma, as is the case of other sarcomas [27–30].

We report here the generation of human cells that overexpress the OCT4/3 gene with physiological co-activator EWS (translation product of the EWS gene). In this study we show that the cells of mesenchymal origin overexpressing OCT4/3 can be traced back to cells with an embryonic phenotype.

Materials and methods

Cell culture

GBS6 cells were generated from primary or first passage cells of a pelvic tumor [31], and cultured in tissue culture dishes (100 mm, Becton Dickinson) in the G031101 medium (Med Shiroto, Tokyo). All cultures were maintained at 37 °C in a humidified atmosphere containing 95% air and 5% CO₂. When the cultures reached subconfluence, the cells were harvested with Trypsin-EDTA Solution (cat# 23315, IBL) at 0.06% trypsin, and replated at a density of 5×10^5 in a 100 mm dish. Medium changes were carried out twice weekly thereafter. Both H4-1 and Yub10F were human bone marrow cells. The 3F0664 were human bone marrow-derived mesenchymal cells and were purchased from Lonza (PT-2501, Basel, Switzerland). The H4-1, Yub10F and 3F0664 cells were cultured in the mesenchymal-stem-cell-growth (MSCG)-Medium-BulletKit (PT-3001, Lonza). The NCR-G1 (a human yolk sac tumor line), NCR-G2 (a human embryonal carcinoma cell line from a testicular tumor), NCR-G3 (a human embryonal carcinoma cell line from a testicular tumor) and NCR-G4 (a human embryonal carcinoma cell line) were cultured in the G031101 medium as previously described [32]. In an experiment to inhibit cell adhesion, GBS6 and NCR-G3 cells were treated with anti-human E-cadherin, monoclonal (Clone HECD-1) (M106, TAKARA BIO INC.) at 100 µg/mL. Treatment with the demethylating agent, 5'-aza-2'-deoxycytidine (5azaC; A2385, SIGMA), was performed on GBS6 cells. GBS6 cells were treated with 3 µM of 5azaC for 24 h, and then cultured without treatment for

24 h. The 5azaC-treated GBS6 cells were described as "GBS6-5azaC". MRC-5 human fetal lung fibroblasts were maintained in POWEREDBY10 medium (MED SHIROTORI CO., Ltd, Tokyo, Japan). We used these cells at between 17 and 25 PDs for the infection of the retroviral vectors. 293FT cells were maintained in DMEM containing 10% FBS, 1% penicillin and streptomycin. iPS cells were maintained in iPSellon medium (007001, Cardio) supplemented with 10 ng/mL recombinant human basic fibroblast growth factor (bFGF, WAKO, Japan). For passaging, iPS cells were washed once with PBS and then incubated with Dulbecco's Phosphate-Buffered Saline (14190-144, Invitrogen) containing 1 mg/mL Collagenase IV (17104-019, Invitrogen), 1 mM CaCl₂, 20% Knockout Serum Replacement (KSR) (10828-028, Invitrogen), and 0.05% Trypsin-EDTA Solution (23315, IBL) at 37 °C. When colonies at the edge of the dish started dissociating from the bottom, DMEM/F12/collagenase was removed. Cells were scraped and collected into 15 mL conical tubes. An appropriate volume of the medium was added, and the contents were transferred to a new dish on irradiated MEF feeder cells. The split ratio was routinely 1:3.

G-banding karyotypic analysis and spectral karyotyping (SKY) analysis

Metaphase spreads were prepared from cells treated with Colcemid (Karyo Max, Gibco Co. BRL, 100 ng/mL for 6 h). We performed a standard G-banding karyotypic analysis on at least 50 metaphase spreads for each population. SKY analysis was performed on metaphase-transduced cells according to the kit manufacturer's instruction (ASI, Carlsbad, CA) and a previously published method [33].

RT-PCR

The cDNAs were synthesized with an aliquot (5 µg) of each total RNA using Oligo-(dT)20 primer (18418-020, Invitrogen) and SuperScript III Reverse Transcriptase (18080-044, Invitrogen). Both the RNA strand of an RNA-DNA hybrid and single-stranded DNA were degraded by RNaseH (18021-071, Invitrogen). For the thermal cycle reactions, cDNA was amplified by T3 Thermocycler (Biometra, Goettingen, Germany) under the following reaction conditions: 30 cycles of a PCR (94 °C for 30 s, 55 °C for 30 s and 72 °C for 30 s) after an initial denaturation (94 °C for 1 min). Primer sets used for PCR reactions are described in Tables 1 and 2. As the same amount of cDNA template was used in all reactions, in comparison to the glyceraldehyde-3-phosphate dehydrogenase (GAPDH) standard, the expression levels were evaluated. The controls consisted of reactions without reverse transcriptase in the process of cDNA synthesis.

Table 1 – PCR primers to detect the chimeric EWS-OCT4/3 gene and untranslocated OCT4/3 gene.

Symbol	Name	Sequence
A	EWS exon6-F	5' TTA GAC CGC AGG ATG GAA AC 3'
B	EWS ex6 intron-F	5' GTG GGG TTC ACT AT 3'
C	POU5F1-1a-F	5' GAT CCT CGG ACC TGG CTA AG 3'
D	POU5F1-2-F	5' CTT GCT GCA GAA GTG GGT GGA GGA A 3'
E	POU5F1-1a-R	5' TCA GGC TGA GAG GTC TCC AA 3'
F	POU5F1-3-R	5' CTG CAG TGT GGG TTT CGG GCA 3'

Table 2 – PCR primers for detection of gene transcripts.

Name	Sequence	Size (bp)
Nanog	Forward: 5' AGT CCC AAA GGC AAA CAA CCC ACT TC 3' Reverse: 5' ATC TGC TGG AGG CTG AGG TAT TTC TGT CTC 3'	164
Sox2	Forward: 5' ACC GGC GGC AAC CAG AAG AAC AG 3' Reverse: 5' GCG CCG CGG CCG GTA TTT AT 3'	253
UTF1	Forward: 5' ACC AGC TGC TGA CCT TGA AC 3' Reverse: 5' TTG AAC GTA CCC AAG AAC GA 3'	230
GAPDH	Forward: 5' GCT CAG ACA CCA TGG GGA AGG T 3' Reverse: 5' GTG GTG CAG GAG GCA TTG CTG A 3'	474

Immunoblot analysis

Whole lysates of GBS6 or NCR-G3 cells were loaded on 10% SDS/PAGE (40 µg total protein/lane) and transferred to a nitrocellulose membrane. The blots were probed with antibodies against anti-Oct3/4 (C-20 for the C-terminus of OCT4/3 of human origin; sc-8629, Santa Cruz), developed with polyclonal rabbit anti-goat Immunoglobulins/HRP antibody (P0160; Dako), and detected by

chemiluminescence following the manufacturer's protocol (ECL Western Blotting Analysis System, Amersham).

Flow cytometric analysis

Cells were stained for 30 min at 4 °C with primary antibodies and immunofluorescent secondary antibodies. The cells were then analyzed on a Cytomics FC 500 (Beckman Coulter, Inc., Fullerton, CA, USA) and the data were analyzed with the FC500 CXP Software ver.2.0 (Beckman Coulter, Inc., Fullerton, CA, USA). Antibodies against human CD9 (555372, PharMingen), CD13 (IM0778, Beckman), CD14 (6603511, Beckman), CD24 (555426, PharMingen), CD29 (6604105, PharMingen), CD31 (IM1431, Beckman), CD34 (IM1250, Beckman), CD44 (IM1219, Beckman), CD45 (556828, PharMingen), CD50 (IM1601, Beckman), CD55 (IM2725, Beckman), CD59 (IMK3457, Beckman), CD73 (550257, PharMingen), CD81 (555676, PharMingen), CD90 (IM1839, Beckman), CD105 (A07414, Beckman), CD106 (IM1244, Beckman), CD117 (IM1360, Beckman), CD130 (555756, PharMingen), CD133 (130-080-801, Miltenyi Biotec), CD135 (IM2234, Beckman), CD140a (556002, PharMingen), CD140b (558821, PharMingen), CD157 (D036-3, IBL), CD166 (559263, PharMingen), CD243 (IM2370, Beckman), ABCG2 (K0027-3, IBL),

Table 3 – Expression of human ES cell-associated genes.

A		OCT4/3	SOX2	NANOG	UTF1	TDGF1	ZIC3	DPPA4	MYC	KLF4
GBS6	Flags	P	A	A	A	A	A	A	P	A
	Raw	2493	56	9	15	23	19	9	3261	171
GBS6-5azaC	Flags	P	A	A	A	A	A	A	P	A
	Raw	6620	146	19	28	20	15	11	1359	102
NCR-G1	Flags	A	A	A	A	P	P	A	A	A
	Raw	46	67	11	19	5180	2349	97	157	91
NCR-G2	Flags	P	A	P	A	P	P	P	A	A
	Raw	2093	120	3972	166	2154	389	873	160	84
NCR-G3	Flags	P	P	P	P	P	P	P	P	P
	Raw	14338	1239	14925	9208	11207	5294	4036	1086	1151
NCR-G4	Flags	P	P	P	P	P	P	P	P	A
	Raw	10602	352	9469	1684	9830	2741	2138	746	151
H4-1	Flags	A	A	A	A	A	A	A	P	P
	Raw	83	13	11	17	40	7	2	1635	489
3F0664	Flags	A	A	A	A	A	A	A	P	P
	Raw	56	63	14	34	21	21	22	735	832
Yub10F	Flags	A	A	A	A	A	A	A	P	A
	Raw	19	49	9	63	12	12	4	680	9
B										
Gene symbol	Probe set ID	Gene name								
POU5F1	208286_x_at	Oct4/3								
SOX2	213721_at	Sox2								
NANOG	220184_at	Nanog; Nanog homeobox								
UTF1	208275_x_at	Utf1; undifferentiated embryonic cell transcription factor 1								
TDGF1	206286_s_at	Tdgf1; teratocarcinoma-derived growth factor 1								
ZIC3	207197_at	Zic3; odd-paired homolog								
DPPA4	219651_at	Dppa4; developmental pluripotency associated 4								
MYC	202431_s_at	c-myc								
KLF4	220266_s_at	Klf4; Kruppel-like factor 4								

A. Gene expression was examined with the Human Genome U133A Probe array (Affymetrix). Raw data values (*Raw*) for each gene expression are shown. *Flags*: Gene expression was judged to be "P (present)" or "A (absent)" in each cell by the GeneChip Analysis Suite 5.0 computer program. GBS6-5azaC: GBS6 cells were exposed to 3 µM 5'-aza-2'-deoxycytidine for 24 h, and then cultured without any treatment for 24 h.

B. Gene names for each symbol.

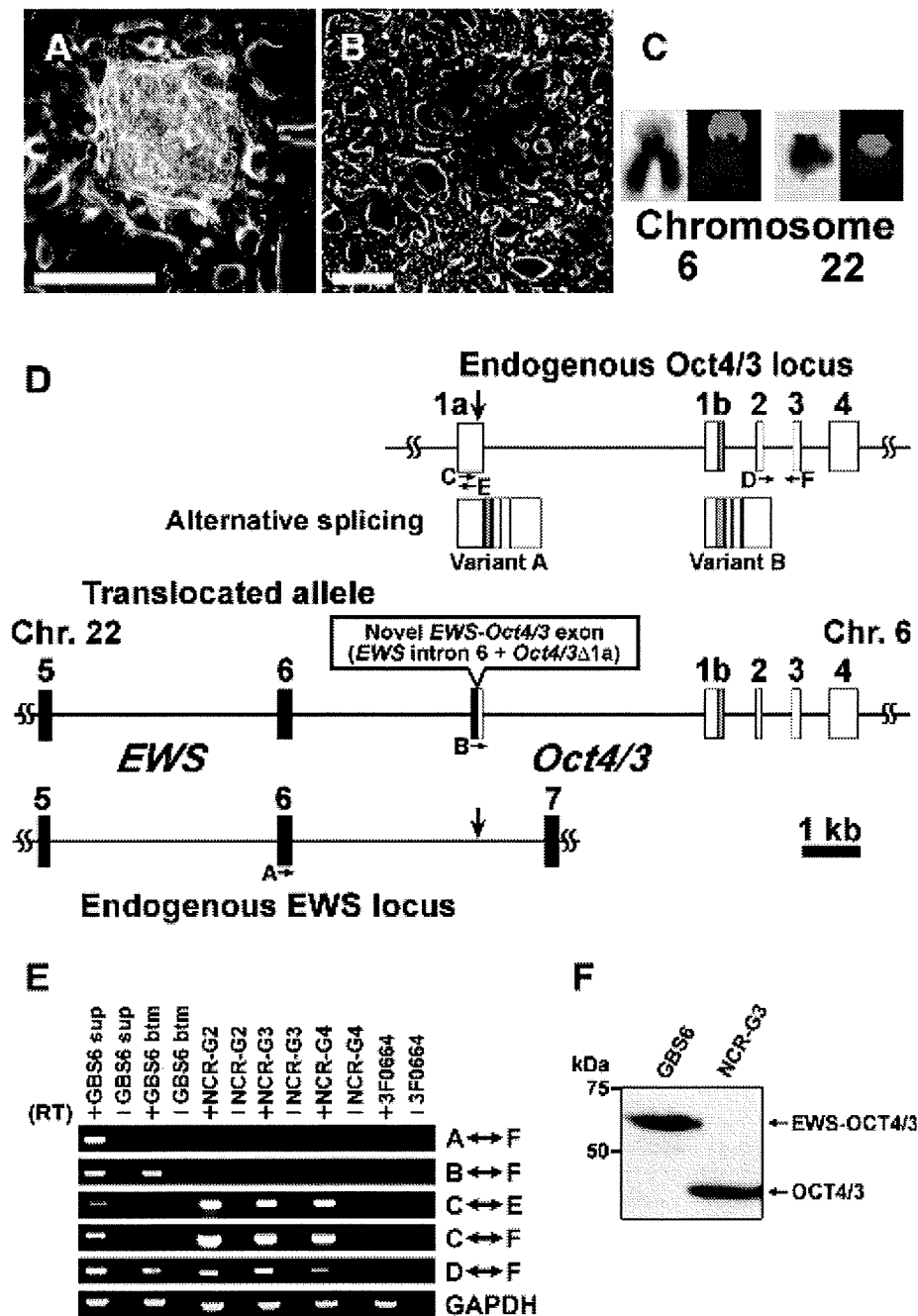


Fig. 1 – Phase contrast micrograph of GBS6 cells, and expression of the translocated *POU5F1/OCT4/3* gene. A cell line termed “GBS6” was generated from primary or first passage cells of a pelvic tumor [31]. (A) GBS6 cell aggregate (GBS6 sup). Scale bar: 100 μ m. (B) GBS6 adherent cells (GBS6 btm). Scale bar: 100 μ m. (C) G-banding karyotypic analysis and Spectral karyotyping (SKY) analysis of the translocated chromosomes. (D) Schematic representation of the *EWS-OCT4/3* structure in the t(6;22) tumor. *EWS* exons are represented by black boxes and *OCT4/3* exons by open boxes. The *OCT4/3*-1b exon is composed of an open and gray box. The novel *EWS-OCT4/3* chimeric exon is created by the fusion between *EWS* intron 6 and part of the exon of *OCT4/3* (Δ 1a). The vertical arrows indicate each breakpoint on either chromosome 22 (*EWS*) or chromosome 6 (*OCT4/3*). The horizontal arrows indicate the position and direction of primers for PCR (Table 1). (E) RT-PCR analysis of the translocated *OCT4/3* gene and the untranslocated *OCT4/3* gene in GBS6 cell, NCR-G2, NCR-G3, NCR-G4, and 3F0664 cells. NCR-G2, NCR-G3, and NCR-G4 cells are embryonal carcinoma cells, and 3F0664 cells are mesenchymal cells. (F) Western blot analysis of *EWS-OCT4/3* in GBS6 cells. Western blot analysis was performed using anti-Oct4/3 antibody. *EWS-OCT4/3* chimeric protein (~58 kDa) was detected in GBS6 cells. The positions of prestained molecular markers (BIO-RAD) are indicated to the left (kDa).

HLA-ABC (IM1838, Beckman), HLA-DR, DP, DQ (6604366, Beckman), SSEA-1 (MAB4301, Chemicon), SSEA-3 (MAB4303, Chemicon), SSEA-4 (MAB4304, Chemicon), STRO-1 (MAB1038, R and D Systems), TRA-1-60 (MAB4360, Chemicon), and TRA-1-81 (MAB4381, Chemicon) were adopted as primary antibodies. PE-conjugated anti-mouse Ig antibody (550589, Pharmingen), PE-conjugated anti-mouse IgM antibody (555584, Pharmingen) and PE-conjugated anti-rat Ig antibody (550767, Pharmingen) were used as secondary antibodies. X-Mean, the sum of the intensity divided by total cell number, was automatically calculated, and it was adopted for the evaluation of this experiment.

Implantation of cells into mice

GBS6 cells ($>1 \times 10^7$) were subcutaneously inoculated into an immunodeficient, NOD/Shi-*scid*, IL-2R γ^{null} mouse (NOG mouse) (CREA, Tokyo, Japan). Subcutaneous specimens were resected at 2 weeks after implantation. The operation protocols were accepted

by the Laboratory Animal Care and the Use Committee of the National Research Institute for Child and Health Development, Tokyo (approval number: 2003-002 and 2005-003).

Immunohistochemistry analysis

Immunohistochemical analysis was performed as previously described [34–36] with antibodies to MIC2 (clone# 12E7, cat# M3601, DAKO, Carpinteria, CA, USA), vimentin (clone# V9, cat# M0725, DAKO, Carpinteria, CA, USA), neurofilament protein 70 kDa (NF-L, clone# 2F11, cat# M0762, DAKO, Carpinteria, CA, USA), desmin (clone# D9, cat# 010031, Bio-Science Products AG, Emmenbruecke, Switzerland), smooth muscle actin (clone# 1A4, cat# M0851, DAKO, Carpinteria, CA, USA), and OCT4/3 (clone# C-10, cat# sc-5279, Santa Cruz Biotechnology, Inc., CA, USA) in PBS containing 1% bovine serum albumin. As a methodological control, the primary antibody was omitted. Immunohistochemical analysis of iPS cells was performed according to the manufacturer's protocol [SCR002,

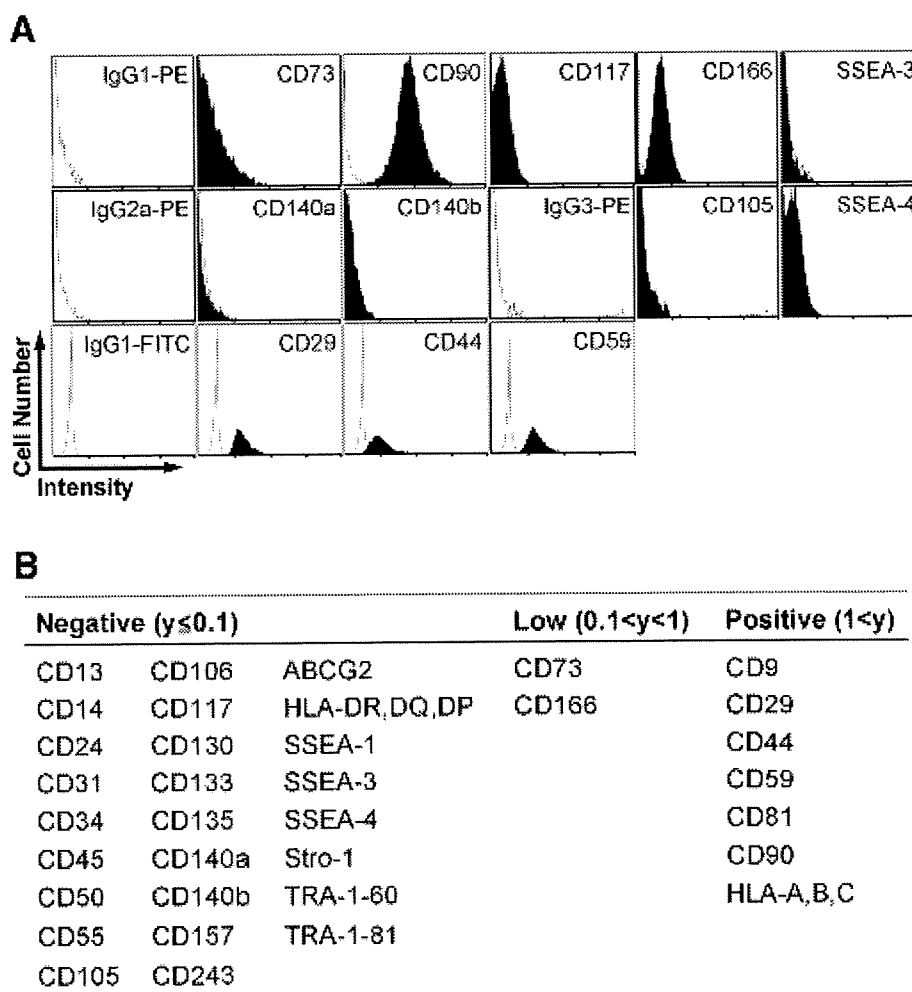
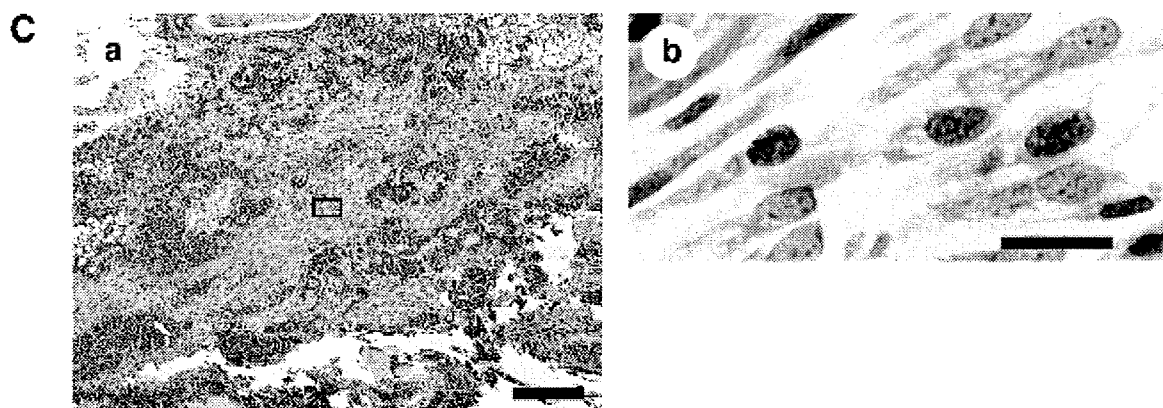
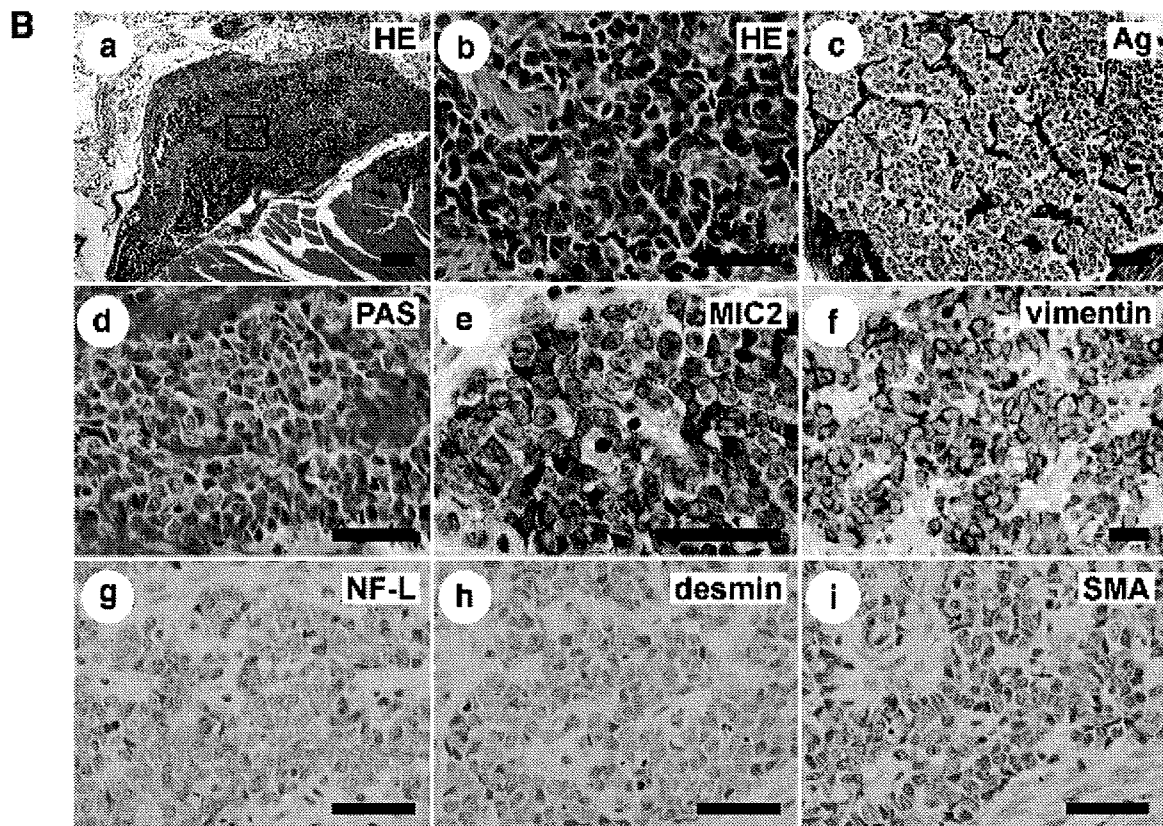
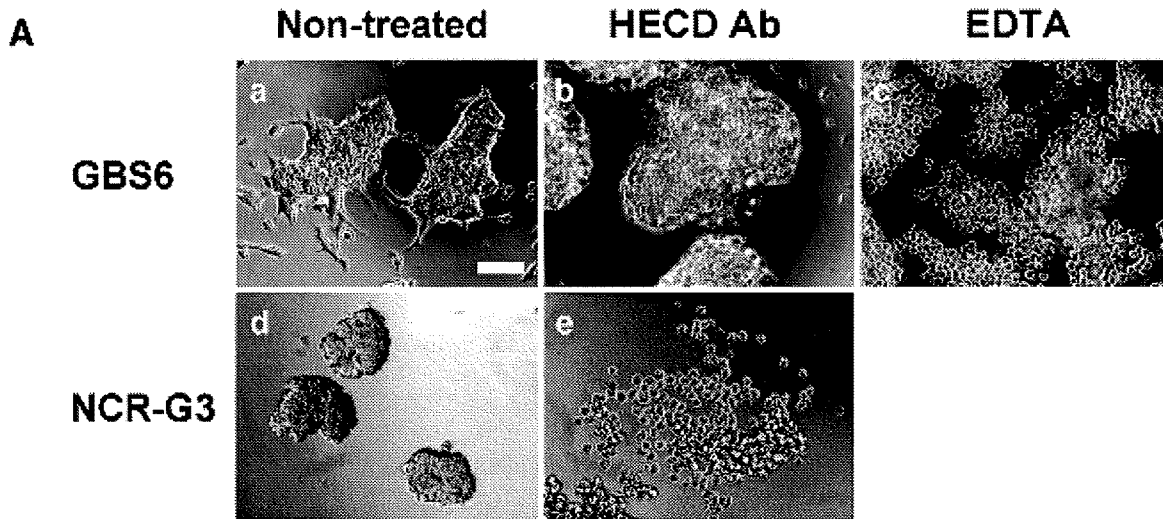


Fig. 2 – Cell surface marker analysis of GBS6 cells. (A) Flow cytometric analysis of cell surface markers in GBS6 cells. The results of CD73, CD90, CD117, CD166 and SSEA-3 were compared with the result of their isotype control, PE-conjugated IgG1. The results of CD140a and CD140b were compared with the result of PE-conjugated IgG2a. The results of CD105 and SSEA-4 were compared with the result of PE-conjugated IgG3. The results of CD29, CD44 and CD59 were compared with the result of FITC-conjugated IgG1. X-axis and Y-axis indicate the intensity and the cell number, respectively. (B) Summary of cell surface markers. “y” is “X-means” subtracted by a value of isotype control; “ $y < 0.1$ ”, “ $0.1 < y < 1$ ”, and “ $1 < y$ ” were determined “negative”, “low” and “positive”, respectively.



Chemicon (Millipore)]. Primary antibodies included Oct-3/4 (C-10) (diluted at 1:300, sc-5279, Santa Cruz), NANOG (diluted at 1:300, RCAB0003P, ReproCELL), SSEA-4 (diluted at 1:300, MAB4304, CHEMICON), and TRA-1-60 (diluted at 1:300, MAB4360, CHEMICON). Secondary antibodies used were Alexa Fluor 546 Goat Anti-mouse IgG, 2 mg/mL (diluted at 1:300, A11003, Invitrogen), Alexa Fluor 488 Goat Anti-rabbit IgG, 2 mg/mL (diluted at 1:300, A11008, Invitrogen), and Alexa Fluor 488 Goat Anti-mouse IgG, 2 mg/mL, F(ab')₂ fragment (diluted at 1:300, A11017, Invitrogen). Nuclei were stained with 1 µg/mL DAPI (40043, Biotium).

Quantitative RT-PCR

RNA was extracted from cells using the RNeasy Plus Mini kit (Qiagen). An aliquot of total RNA was reverse transcribed by using an oligo (dT) primer. For the thermal cycle reactions, the cDNA template was amplified (ABI PRISM 7900HT Sequence Detection System) using the Platinum Quantitative PCR SuperMix-UDG with ROX (11743-100, Invitrogen) under the following reaction conditions: 40 cycles of PCR (95 °C for 15 s and 60 °C for 1 min) after an initial denaturation (95 °C for 2 min). Fluorescence was monitored during every PCR cycle at the annealing step. The authenticity and size of the PCR products were confirmed using a melting curve analysis (using software provided by Applied Biosystems) and a gel analysis. mRNA levels were normalized using *GAPDH* as a housekeeping gene. POU5F1-2-F and POU5F1-3-R primers were used to detect the *OCT4/3* gene (see Table 1, D and F).

Chromatin immunoprecipitation (ChIP) assays

Chromatin immunoprecipitation was performed according to the instructions of the EZ ChIP Chromatin Immunoprecipitation Kit (17-371, Upstate Biotechnology Inc., Chicago, IL, USA). Histone and DNA were cross-linked with 1% formaldehyde for 10 min at room temperature and formaldehyde was then inactivated by the addition of 125 mM glycine. The chromatin was then sonicated to an average DNA fragment length of 200 to 1000 bp. Soluble chromatin reacted with and without anti-acetylated Histone H3 (06-599, Upstate Biotechnology Inc., Chicago, IL, USA), and anti-acetylated Histone H4 (06-866, Upstate Biotechnology Inc., Chicago, IL, USA). The immunocomplex was purified and collected in elution buffer (0.1 M NaHCO₃, 1% sodium dodecyl sulfate). Crosslinking was then reversed using elution buffer containing RNase A (0.03 mg/mL) and NaCl (0.3 M) by incubation for 4 h at 65 °C. Supernatant obtained without antibody was used as the input control. The DNA was treated with proteinase K for 1 h at 45 °C and purified. For all ChIP experiments, quantitative PCR analyses were performed in real time as described in this manuscript. Relative

occupancy values were calculated by determining the apparent immunoprecipitation efficiency (ratios of the amount of immunoprecipitated DNA to that of the input sample) and normalized to the level observed at a control region. For all the primers used, each gave a single product of the right size adult stem cell confirmed by agarose gel electrophoresis and dissociation curve analysis. These primers also gave no DNA product in the no-template control. The following three primer sets for human *OCT4/3*, as previously described [26], were adopted for real-time PCR to quantitate the ChIP-enriched DNA: human *POU5F1-A* (-2613/-2396), 5'-GGG GAACCTGGAGGATGG-CAAGCTGAGAAA-3' and 5'-GGCCTGTGGGGGTGGGAGG AACAT-3'; human *POU5F1-B* (-1779/-1563), 5'-CCTGCACCCCTCCACAAATCACTC GC-3' and 5'-TGCAATCCCCTCAAAGACTGAGCCTCAGAC-3'; human *POU5F1-C* (-237/-136), 5'-GAGGGGCGCCAGTTGTGTCTCCCGTTT-3' and 5'-GGGAGGTGGG GGGAGAACTGAGCCGAAGG-3'.

DNA methylation analysis

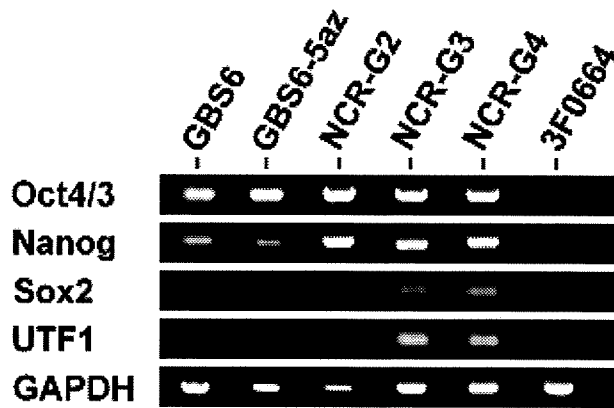
The NCR-G2 (JCRB cell bank number; JCRB1167) [32], NCR-G3 (JCRB cell bank number; JCRB1168) [32], GBS6, and Yub636BM (human bone marrow cells derived from an extra digit) cells were prepared for this assay. Genomic DNA was isolated using DNeasy Blood and Tissue Kit (69504, QIAGEN). Primers were selected from the CpG island regions with homogenous CpG site methylation patterns. The target region of the genes used for methylation analysis and the primer sequences used for PCR amplification are shown in Table 4. One of the two primers in the PCR amplification of the target regions is tagged with a T7 promoter sequence: cagtaatcagactactataggagaaggct. The PCR reactions were carried out in a total volume of 5 µL using 1 pmol of each primer, 40 µM dNTP, 0.1 U HotStar Taq DNA polymerase (QIAGEN), 1.5 mM MgCl₂, 5× PCR buffer (final concentration 1×), and bisulfite-converted DNA. The reaction mix was preactivated for 15 min at 95 °C. The reactions were amplified in 45 cycles of 95 °C for 20 s, 62 °C for 30 s, and 72 °C for 30 s followed by 72 °C for 3 min. Unincorporated dNTPs were dephosphorylated by adding 1.7 µL DNase-free water and 0.3 U Shrimp Alkaline Phosphatase (SAP). The reaction was incubated at 37 °C for 20 min and SAP was then heat-inactivated for 10 min at 85 °C. Typically, 2 µL of the PCR reaction was directly used as a template in a 6.5 µL combined transcription-cleavage reaction. Twenty units of T7 polymerase (Epicentre) were used to incorporate either dCTP or dTTP in the transcripts. Ribonucleotides at 1 mM and the dNTP substrate at 2.5 mM were used. RNase A (Sequenom) was included to cleave the in vitro transcript. The mixture was then further diluted with water to a final volume of 27 µL. Conditioning of the phosphate backbone prior to MALDI-TOF MS was achieved by the addition of 6 mg CLEAN resin (Sequenom). The cleavage reaction samples (15 nL) were dispensed onto silicon

Fig. 3 – In vitro and in vivo characteristics of GBS6 cells. (A) Ca⁺⁺-dependent, E-cadherin-independent adhesion of GBS6 cell aggregates. GBS6 cells (a) were unaffected by the antibody to E-cadherin (b), but were dissociated by EDTA, Ca⁺⁺ chelator (c). In contrast, NCR-G3 cells (d), serving as a control since they are E-cadherin-dependent, were dissociated and induced to death by the antibody to E-cadherin (e). Scale bar: 100 µm. (B) Immunohistochemical analysis of GBS6 cells implanted into the subcutaneous tissue of NOG mice. GBS6 cells at 2 weeks after implantation (a, b: hematoxylin and eosin stain, c: silver stain, d: PAS stain) were examined for immunohistochemical analysis using antibodies to MIC2 (e), vimentin (f), neurofilament protein 70 kDa (g: NF-L), desmin (h), and smooth muscle actin (i: SMA). Scale bars: 200 µm (a) and 50 µm (b–i). (C) Immunohistochemical analysis with the anti-OCT4/3 antibody of GBS6 cells implanted into the subcutaneous tissue of NOG mice. GBS6 cells at 2 weeks after implantation were examined for immunohistochemical analysis using antibodies to OCT4/3. The higher-magnification image of the region enclosed by a square in “a” (b). Scale bars: 200 µm (a) and 20 µm (b).

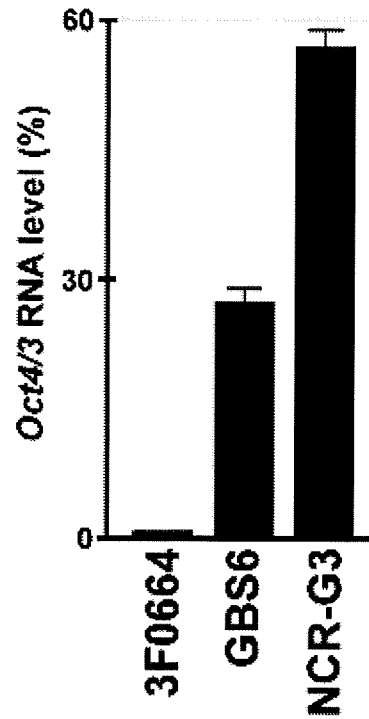
chips preloaded with matrix (SpectroCHIP, Sequenom). Mass spectra were collected using a MassARRAY mass spectrometer (Sequenom). Spectra were analyzed using proprietary peak picking and spectra interpretation tools (EpiTYPER, Sequenom).

For analysis of DNA methylation, we examined the methylation-dependent C/T sequence changes introduced by bisulfite treatment. Those C/T changes are reflected as G/A changes on the reverse strand and hence result in a mass difference of 16 kDa for

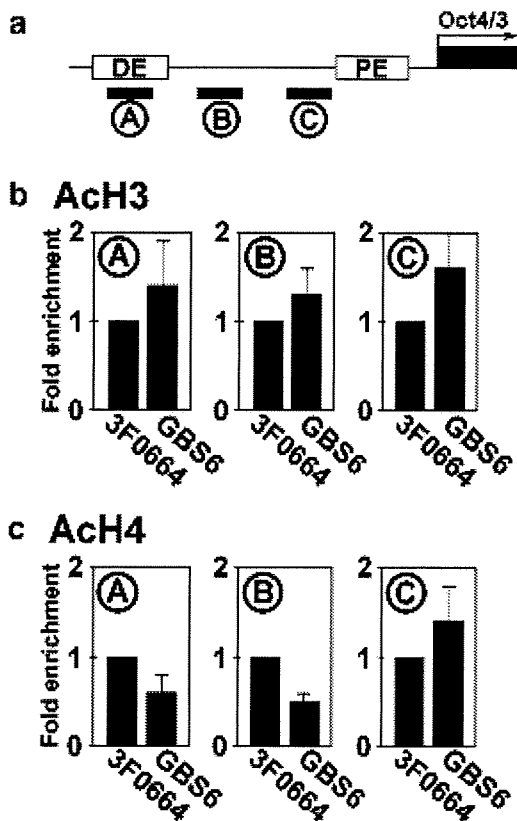
A



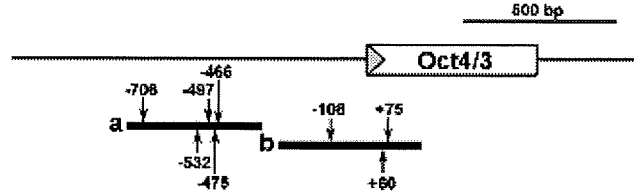
B



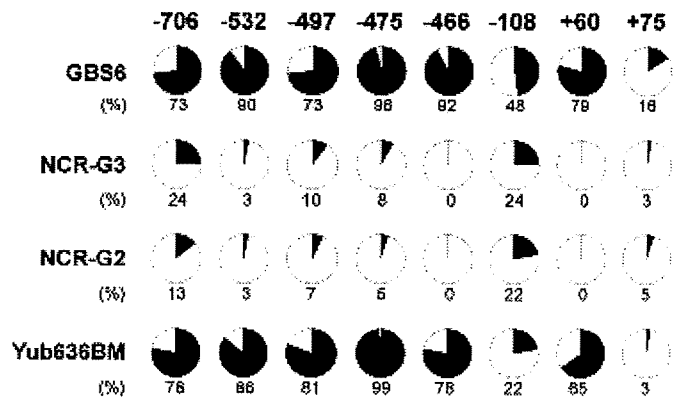
C



D



E



each CpG site enclosed in the cleavage products generated from the RNA transcript. The mass signals representing nonmethylated DNA and those representing methylated DNA, built signal pairs, which are representative for the CpG sites within the analyzed sequence substrings. The intensities of the peaks were compared, and the relative amount of methylated DNA was calculated from this ratio. The method yields quantitative results for each of these sequence-defined analytic units referred to as CpG units, which contain either one individual CpG site or an aggregate of subsequent CpG sites.

Plasmid construction

Each open reading frame of human *OCT4/3* and *SOX2* was amplified by RT-PCR using the RNA extracted from NCR-G2 cells (JCRB cell bank number: JCRB1167) [32], a complex-type germ cell tumor cell line. Also, those of *c-MYC* and *KLF4* were amplified by RT-PCR using the RNA extracted from the bone marrow stromal cell line, UET13. A Gateway cassette composed of an attR1/R2 flanked CmR and ccdB (Invitrogen) was amplified by PCR and ligated into the Eco RI/Not I site of pMXs retroviral expression vector to create pMXs-DEST [37]. PCR amplification was performed by using KOD-Plus-DNA polymerase (KOD-201, TOYOBO). The constructs were confirmed by sequencing.

Retroviral infection and iPS cell generation

293FT cells (Invitrogen) were plated at 2×10^6 cells per 100 mm dish and incubated overnight. The next day, the cells were co-transfected with pMXs-*OCT4/3*, pMXs-*SOX2*, pMXs-*c-MYC*, pMXs-*KLF4*, pCL-GagPol, and pHCMV-VSV-G vectors with TransIT-293 reagent (Mirus, Madison, WI). Twenty-four hours after transfection, the medium was replaced with a new medium, which was collected after 48 h as the virus-containing supernatant. MRC-5 cells were seeded at 1×10^5 cells per 35 mm dish 1 day before infection. The virus-containing supernatants were filtered through a 0.45 μm pore-size filter, ultracentrifuged at 8500 rpm for 16 h, and then resuspended in DMEM (D6429, SIGMA) supplemented with 4 mg/mL polybrene (Nacalai Tesque). Equal amounts of concentrated supernatants containing each of the four retroviruses were mixed, transferred to MRC-5 cells, and incubated for 8 h. The MRC-5 cells were cultured for 4 days and replated on an irradiated MEF feeder layer in 100 mm dish. The medium was replaced with the

iPSellon medium supplemented with 10 ng/mL bFGF. One-half of the medium was changed every day and the cells were cultured up to 30 days after a day of infection. Colonies were picked up and transferred into 0.2 mL of iPSellon medium when colonies appeared. The colonies were mechanically dissociated to small clumps by pipeting up and down or mechanically cut using a STEMPRO EZPassage disposable passaging tool (23181010, Invitrogen). The cell suspension was transferred on irradiated MEF feeder in 4-well plates [176740, Nunc (Thermo Fisher Scientific)]. We define this stage as passage 1.

Teratoma formation

iPS cells were harvested by accutase treatment, collected into tubes, and centrifuged, and the pellets were suspended in the iPSellon medium. The same volume of Basement Membrane Matrix (354234, BD Biosciences) was added to the cell suspension. Cells (1×10^7) were implanted subcutaneously to a BALB/c-*nu/nu* mouse (CREA, Japan) for 4 weeks. Tumors were dissected and fixed with PBS containing 4% paraformaldehyde. Paraffin-embedded tissue was sliced and stained with hematoxylin and eosin.

GeneChip expression analysis

Total RNA was extracted from cells using the RNeasy Mini Kit (74104, Qiagen, Valencia, CA). Genomic DNA was eliminated by DNase I (2215A, TAKARA BIO INC.) treatments. From all RNA samples, 5 μg of total RNA was used as a starting material for the microarray sample preparation. Double-stranded cDNA was synthesized from DNase-treated total RNA, and the cDNA was subjected to in vitro transcription in the presence of biotinylated nucleoside triphosphates using the Enzo BioArray HighYield RNA Transcript Labeling Kit (Enzo Life Sciences, Inc., Farmingdale, NY), according to the manufacturer's protocol (One-Cycle Target Labeling and Control Reagent package). Human-genome-wide gene expression was examined with the Human Genome U133A Probe array (GeneChip, Affymetrix), which contains the oligonucleotide probe set for approximately 23,000 full-length genes and expressed sequence tags (ESTs), according to the manufacturer's protocol (Expression Analysis Technical Manual and GeneChip small sample target labeling Assay Version 2 technical note, <http://www.affymetrix.com/support/technical/index.affx>) as previously described [5]. Hierarchical clustering and principle component

Fig. 4 – Expression of the *OCT4/3* gene and histone modification of the *OCT4/3* promoter in GBS6 cells. (A) Expression of embryonic stem cell-enriched genes in GBS6, NCR-G2, NCR-G3, NCR-G4, and 3F0664 cells. GBS6 cells expressed the *OCT4/3* and *NANOG* genes, but not the *SOX2* and *UTF1* genes. NCR-G2 cells expressed the *OCT4/3* and *NANOG* genes; both NCR-G3 cells and NCR-G4 cells expressed the *OCT4/3*, *NANOG*, *SOX2* and *UTF1* genes. 3F0664 mesenchymal cells did not express these four kinds of embryonic stem cell-enriched genes. *POU5F1-1a-F* and *POU5F1-1a-R* (Table 1) were used to amplify the endogenous *OCT4/3* gene. (B) Quantitative PCR analysis to assess the expression level of *OCT4/3* mRNA in GBS6. *OCT4/3* mRNA level is expressed relative to 3F0664 cells control. (C) Real-time PCR to quantitate the ChIP-enriched DNA using acetylated Histone H3 and acetylated Histone H4 antibodies. Schematic of the location of the amplicons (A–C) used to detect ChIP-enriched fragments in *OCT4/3* shown relative to the distal enhancer (DE)/CR4 region, to the proximal enhancer (PE), and to transcription start site (arrow) (a). The relative levels of acetylated Histone H3 (b) and acetylated Histone H4 (c) modifications were detected in GBS6 cells and 3F0664 cell control. GBS6 cells are represented by black bars and 3F0664 cells by open bars. (D) DNA methylation analysis in the promoter region of the *OCT4/3* gene. The target regions of *OCT4/3* used for the quantitative DNA methylation analysis. Region 'a' and Region 'b' include 5 (–706, –532, –497, –475, –466) and 3 (–108, +60, +75) CpG sites, respectively. The positions of CpG sites are relative to the *OCT4/3* transcription start site (gray triangle). (E) The relative amount of methylated DNA ratio (%) at each CpG site is indicated as the black area in the pie chart.

analysis were performed to group mesenchymal cells obtained from bone marrow into subcategories (<http://lgsun.grc.nia.nih.gov/ANOVA/>).

Results

Establishment of human cells of mesenchymal origin with overexpression of the translocated *POU5F1/OCT4/3* gene

To investigate whether cells of mesenchymal origin acquire an embryonic phenotype, a novel human cell line termed GBS6 was established from the pelvic bone tumor, of which histology shows diffuse proliferation of undifferentiated tumor cells with oval nuclei and scant but short spindle cytoplasm [31]. The generated cells grew attached to the dish as a polygonal cell sheet with cell aggregates forming in the center (Figs. 1A, B), and retained the reciprocal translocation, t(6; 22), detected in the original tumor (Fig. 1C). The *EWS-OCT4/3* chimeric gene expression also remained (Figs. 1D, E and Table 1). Embryonal carcinoma (EC) cells, i.e., NCR-G2, NCR-G3, and NCR-G4, served as control cells expressing the endogenous *OCT4/3* gene. Immunoblot analysis revealed that *EWS-OCT4/3* fusion protein was expressed in GBS6 cells (Fig. 1F).

Cell surface markers of GBS6 cells

GBS6 cell surface markers were evaluated by flow cytometric analysis (Fig. 2). The results showed that GBS6 cells were strongly positive (Positive; Fig. 2B) for CD9, CD29 (integrin β 1), CD44, CD59, CD81, CD90 (Thy-1) and HLA-A,B,C (HLA class I); weakly positive (Low; Fig. 2B) for CD73 and CD166 (ALCAM); negative (Negative; Fig. 2B) for CD55, CD105 (endogrin), CD140a (PDGFR α), and CD140b (PDGFR β). The lack of CD13, CD55, CD105, CD106, CD140a, and CD140b in GBS6 cells suggests that the surface markers of GBS6 cells are different from those of conventional mesenchymal cells [10,38,39].

E-cadherin-independent growth of GBS6 cells

To investigate whether GBS6 cells survive dependent on E-cadherin-like human embryonic cells, the cells were treated by an inhibitory antibody to E-cadherin (HECD Ab) and EDTA (Fig. 3A). GBS6 cell survival was unaffected by the E-cadherin antibody but affected by EDTA (Fig. 3A-a, b, c). In contrast, NCR-G3 cells, human embryonal carcinoma cells that proliferate in an E-cadherin-dependent manner, were dissociated and induced to apoptosis by the E-cadherin antibody (Fig. 3A-d, e).

Implantation of GBS6 cells into immunodeficient mice

To investigate an in vivo phenotype of GBS6 cells, the cells were intramuscularly injected into immunodeficient NOG mice and examined by histopathology and immunohistochemistry (Fig. 3B). The injected cells exhibited an undifferentiated phenotype with oval nuclei and scant spindle cytoplasm (Fig. 3B-b), and showed an alveolar configuration (Fig. 3B-c). The cells were negative by the PAS stain (Fig. 3B-d). The cells were immunohistochemically positive for MIC2 and vimentin (Fig. 3B-e, f), and negative for neurofilament, desmin, and smooth muscle actin

(Fig. 3B-g, h, i). The cells retained *OCT4/3* in their nuclei even after implantation (Fig. 3C).

Expression of ES-enriched genes

To determine if GBS6 cells express ES cell-enriched genes, that is, the *OCT4/3*, *NANOG*, *SOX2*, and *UTF1* genes, RT-PCR with specific primer sets (Table 2) and gene chip analyses were performed. GBS6 cells expressed the endogenous *OCT4/3* and *NANOG* genes like NCR-G2, NCR-G3, and NCR-G4 embryonal carcinoma cells, but did not express the *SOX2* and *UTF1* genes (Fig. 4A). The results of the RT-PCR analysis were compatible with those of the gene chip analysis (GSE8113, Table 3). To compare the expression level of stem cell-specific genes in GBS6 cells, ES cells, and mesenchymal cells, we performed a quantitative RT-PCR analysis. The expression level of *OCT4/3* was about half that of human EC cells, but was more than twenty-five times that of 3F0664 mesenchymal cells (Fig. 4B). The results show that the expression level of *OCT4/3* is comparable to that of human EC cell.

To determine if the cis-regulatory element of the *OCT4/3* gene has so-called open chromatin structure, we performed the chip analysis using antibodies to acetylated H3 and acetylated H4 (Fig. 4C). The results show that acetylated histone levels which the *OCT4/3* promoter is wrapped around in GBS6 cells are comparable with those in 3F0664 mesenchymal cells. We also performed methylation analysis of the *OCT4/3* gene in GBS6 cells because the expression of *OCT4/3* gene is regulated by methylation (Figs. 4D, E and Table 4). The promoter region of the *OCT4/3* gene was heavily methylated in GBS6 cells as compared with human NCR-G3 embryonal carcinoma cells expressing the *OCT4/3* gene at a high level.

Cell reprogramming assay

To investigate if chimeric *EWS-OCT4/3* induces iPS cells like native *OCT4/3*, we performed Yamanaka's reprogramming assay on MRC-5 human fetal lung fibroblasts (Fig. 5A), using the chimeric *EWS-OCT4/3* construct with the *KLF-4*, *SOX2*, and *c-MYC* genes according to the conventional protocol [40] with some modifications. We failed to obtain iPS cells using the *EWS-OCT4/3*, *KLF-4*, *SOX2*, and *c-MYC* constructs (Fig. 5B), albeit trials of three independent experiments, whereas, for a control, we successfully generated 101 clones of iPS cells from MRC-5 cells using the *OCT4/3*, *KLF-4*, *SOX2*, and *c-MYC* constructs (Fig. 5C). The iPS cells generated from MRC-5 cells expressed human ES cell-specific surface antigens (Figs. 5D–G). In vivo implantation analysis showed that iPS cells generated various tissues including neural tissues (Fig. 5H: ectoderm), cartilage (Fig. 5I: mesoderm),

Table 4 – Primers used for PCR amplification of the bisulfite-converted DNA.

Name	Sequence	Size (bp)
Region 'a'	Forward: 5' TTG GTT ATT GTG TTT ATG GTT GTT G 3' Reverse: 5' TAA ACC AAA ACA ATC CTT CTA CTC C 3'	437
Region 'b'	Forward: 5' TTT GGG TAA TAA AGT GAG ATT TTG TTT 3' Reverse: 5' CTA ACC CTC CAA AAA AAC CTT AAA A 3'	452

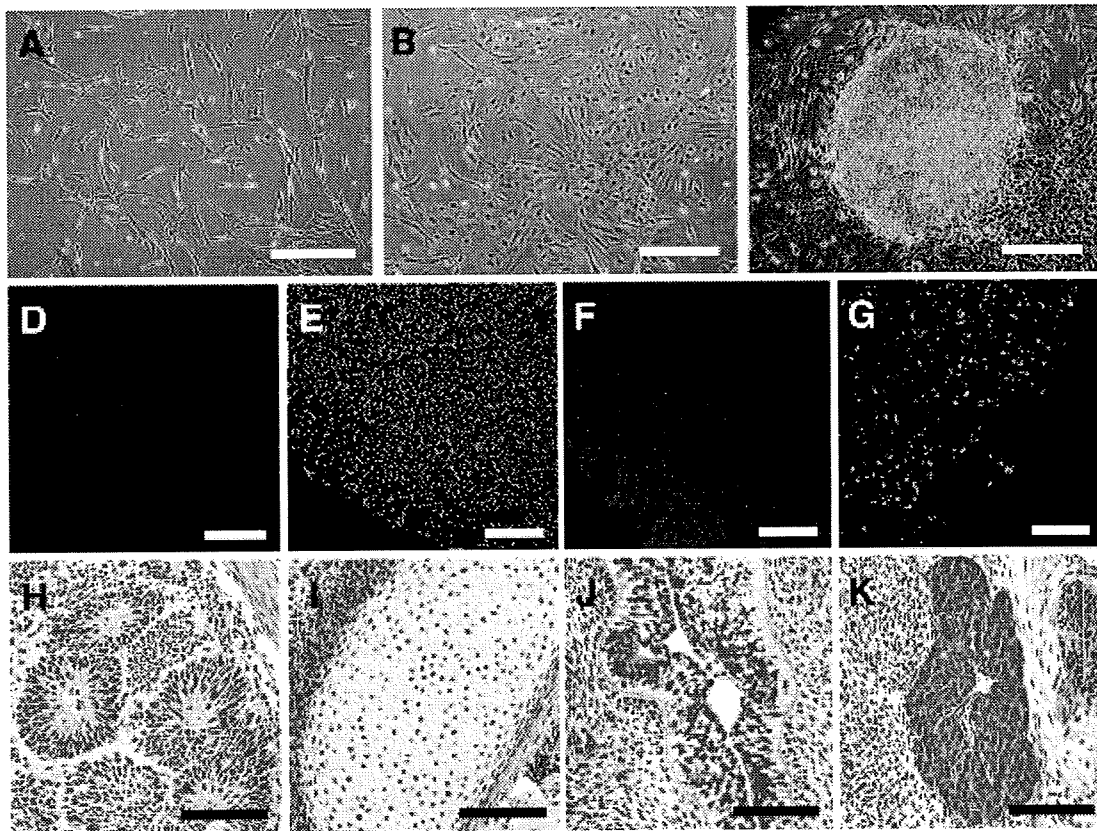


Fig. 5 – Induction of iPS cells from MRC-5 cells and teratoma formation. (A) Morphology of MRC-5 cells. (B) Morphology of cells using *EWS-OCT4/3*, *KLF-4*, *SOX2*, and *c-MYC* genes at Day 30 after infection. (C) Morphology of established iPS cell (clone 16: Fetch) colony using *OCT4/3*, *KLF-4*, *SOX2*, and *c-MYC* genes at Day 20 after infection. (D–G) Immunocytochemistry for OCT4/3 (D), NANOG (E), SSEA-4 (F), and TRA-1-60 (G). Nuclei were stained with DAPI. Bars = 500 μm (A–C), and 200 μm (D–G). In addition, chromosomal G-band analyses showed that human iPS cells from MRC-5 had a normal karyotype of 46XY (not shown). The analysis of short tandem repeat shows that novel iPS cells from MRC-5 cells were not a result of cross-contamination. Hematoxylin and eosin staining of teratoma derived from the generated iPS cells. Cells (1×10^7) were implanted subcutaneously to a BALB/c-*nu/nu* mouse for 4 weeks. Histological examination showed that the tumor contained various tissues, neural tissues (H; ectoderm), cartilage (I; mesoderm), a gut-like epithelial tissue (J; endoderm), and a hepatic tissue (K; endoderm). Bars = 100 μm (H–K).

a gut-like epithelial tissue (Fig. 5J; endoderm), and a hepatic tissue (Fig. 5K; endoderm). These results imply that the chimeric *EWS-OCT4/3* gene does not participate in reprogramming of somatic cells.

Principle component analysis of global gene expression in GBS6 cells

To determine whether GBS6 cells are categorized into embryonal cells or mesenchymal cells, global gene expression patterns of GBS6 cells, embryonal carcinoma cells (NCR-G2, NCR-G3, and NCR-G4), yolk sac tumor cells (NCR-G1), and marrow stromal cells (3F0664, H4-1, and Yub10F) were further analyzed by principle component analysis (PCA), which reduces high-dimensionality data into a limited number of principle components (Fig. 6). The first principle component (PC1) captures the largest contributing factor of variation, which characterizes the differential expression of genes. As we were interested in the differential gene expression component, we plotted the position of each cell type against the PC1, PC2, and PC3 axis in three-dimensional space by using virtual reality modeling language

(Fig. 6A). Close examination of the 3D model identified PC1 as the most representative view of the 3D model. PC1 axis direction is therefore used to characterize the differential gene expression (Fig. 6B). In addition, hierarchical analysis of the cells analyzed for global gene expression revealed that GBS6 cells are categorized into embryonal carcinoma cells and yolk sac tumor cells, i.e., NCR-G1, -G2, -G3, and -G4 cells (Fig. 6C).

Discussion

In this study, we generated a cell line with a transitional form between mesenchymal cells and embryonic stem cells. Loss of mesenchyme-specific cell markers, i.e., CD13, CD55, CD105, CD106, CD140a and CD140b, and modification of cell survival with the calcium chelator indicate that GBS6 cells are no longer mesenchymal cells. Global and drastic differences in gene expression with the GeneChip analysis support the conclusion that GBS6 cells no longer exhibit the profile of mesenchymal cells. It is also noteworthy that this transition phenotype is reliably inherited *ex vivo* after a series of *in vitro* passages.

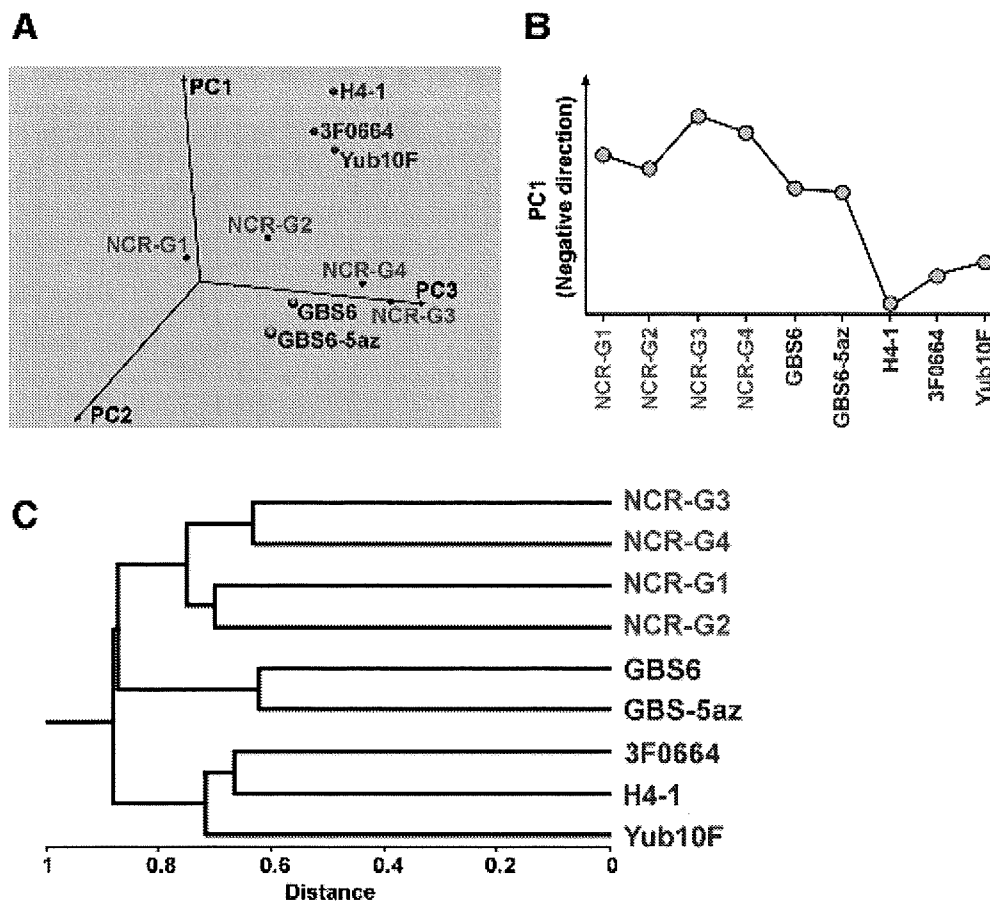


Fig. 6 – Principal component analysis and hierarchical clustering of gene expression in GBS6 cells, embryonic carcinoma cells, and bone marrow cells. (A) 3D-representation of principle component analysis. (B) Principal components of PC1 axis, negative direction. (C) Hierarchical clustering analysis of averages.

OCT4/3 function and its physiological partner EWS in embryonic transition

ES-like cells or iPS cells are generated from murine fibroblasts by transfecting four genes, i.e., *OCT4/3*, *SOX2*, *KLF-4* and *c-MYC* are necessary for the mesenchymal–embryonic transition [1–3]. However, *OCT4/3* alone is not sufficient to confer embryonic phenotypes to human bone marrow-derived cells, NIH3T3 cells (data not shown) or embryonic fibroblasts [1]. *EWS* and *OCT4/3* are directly bound both in vitro and in vivo [41]; in other words, *EWS* is a binding partner of *OCT4/3*. Therefore, the *EWS-OCT4/3* protein in GBS6 cells is considered a fusion between physiological partners. *EWS* and *OCT4/3* are co-expressed in the pluripotent mouse and human ES cells. To investigate if the *EWS-OCT4/3* has a transcriptional activity, we performed the luciferase assay. The results show that the chimeric *EWS-OCT4/3* gene has comparable or higher transcriptional activity than the native *OCT4/3* gene does (Supplementary Fig. S1). Ectopic expression of non-chimeric *EWS* enhances the transactivation activity of *OCT4/3*; the N-terminal QSY domain of *EWS* and the C-terminal POU domain function as a transcriptional activation and DNA binding, respectively [42,43]. The *OCT4/3* gene is overexpressed under the cis-regulatory element of the *EWS* gene [31], and the functional co-operation of *OCT4/3* and *EWS* at a protein level to transcriptional activation may

lead to embryonic transformation in GBS6 cells. Converting mesenchymal cells to embryonic cells opposes the usual direction of ES cell differentiation [44]; and this is achieved by chimeric *OCT4/3* with physiological co-activator *EWS* driven by the potent cis-regulatory element of the *EWS* gene [31]. This phenotypic conversion requires the molecular reprogramming of mesenchymal cells with new instructions.

Mesenchymal to embryonic “incomplete” transition by overexpression of chimeric OCT4/3

OCT4/3 fused to *EWS* not only participates in oncogenesis [29,31], but also contributes to mesenchymal–embryonic transition, at least in part from the viewpoint of global gene expression profiles and cell surface markers (Figs. 2 and 6). GBS6 cells are subcategorized into groups of cells derived from testicular germ cell tumors (Fig. 6A, cells with embryonic phenotypes are shown in pink), and the PC1 axis indicates transition from mesenchymal cell group to embryonic cell group (Fig. 6B). This transition was, however, incomplete; some of the ES-specific genes were not reactivated. *OCT4/3* is a member of the POU family of transcription factors, is expressed in pluripotent ES cells, including primordial germ cells [17–21], and functions as a master switch in differentiation by regulating cells that have, or can develop, pluripotent

potential. However, tight chromatin structure in GBS6 cells may render OCT4/3 recognition sequences inaccessible [45]. The OCT4/3 recognition sequences have been found in the cis-regulatory elements of the FGF-4 and CD140a/platelet-derived growth factor receptor- α gene [46], but GBS6 cells are indeed negative for CD140a (Fig. 2B). Alternatively, the lack of other essential transcription factors such as SOX2 and UTF1 (Fig. 4A, Table 3) and/or co-factors may be a cause of “incomplete” transition. Interestingly, this transition phenotype is reliably inherited *ex vivo* after a series of *in vitro* passages, and this may also be attributed to the function of OCT4/3 that is critical for self-renewal of embryonic stem cells [24].

Mesenchymal to epithelial transition is observed in physiological and pathological conditions [47–50]. In contrast, mesenchymal-embryonic transition has been achieved in an artificial experimental condition *in vitro* [1–3]. Homogenous positive staining for OCT4/3 in embryonal carcinoma cells supports the model that the encoded protein is crucial, and the absence of OCT4/3 in non-embryonal carcinoma cells is in agreement with the inability to generate pluripotent stem cells [51]. The cell line generated in this study with overexpression of chimeric OCT4/3, although this is just one case of rare human immortalized cells, provides us with insight into cell plasticity involving OCT4/3 that is essential for ES cell maintenance and into the complexity required for changing cellular identity.

Acknowledgments

We would like to express our sincere thanks to Michiyo Nasu for histological analysis, Yoriko Takahashi for data mining, and Kayoko Saito for secretary work. This study was supported by grants from the Ministry of Education, Culture, Sports, Science and Technology (MEXT) of Japan and Health and Labor Sciences Research Grants; by Research on Health Science Focusing on Drug Innovation from the Japan Health Science Foundation; by the Program for Promotion of Fundamental Studies in Health Science of the Pharmaceuticals and Medical Devices Agency; by the grant from Terumo Life Science Foundation; by a research Grant for Cardiovascular Disease from the Ministry of Health, Labor and Welfare; and by a Grant for Child Health and Development from the Ministry of Health, Labor and Welfare.

Appendix A. Supplementary data

Supplementary data associated with this article can be found, in the online version, at doi:10.1016/j.yexcr.2009.06.016.

REFERENCES

- [1] K. Takahashi, S. Yamanaka, Induction of pluripotent stem cells from mouse embryonic and adult fibroblast cultures by defined factors, *Cell* 126 (2006) 663–676.
- [2] K. Okita, T. Ichisaka, S. Yamanaka, Generation of germline-competent induced pluripotent stem cells, *Nature* 448 (2007) 313–317.
- [3] M. Wernig, A. Meissner, R. Foreman, T. Brambrink, M. Ku, K. Hochedlinger, B.E. Bernstein, R. Jaenisch, *In vitro* reprogramming of fibroblasts into a pluripotent ES-cell-like state, *Nature* 448 (2007) 318–324.
- [4] M.J. Go, C. Takenaka, H. Ohgushi, Forced expression of Sox2 or Nanog in human bone marrow derived mesenchymal stem cells maintains their expansion and differentiation capabilities, *Exp. Cell Res.* 314 (2008) 1147–1154.
- [5] T. Mori, T. Kiyono, H. Imabayashi, Y. Takeda, K. Tsuchiya, S. Miyoshi, H. Makino, K. Matsumoto, H. Saito, S. Ogawa, M. Sakamoto, J. Hata, A. Umezawa, Combination of hTERT and bmi-1, E6, or E7 induces prolongation of the life span of bone marrow stromal cells from an elderly donor without affecting their neurogenic potential, *Mol. Cell Biol.* 25 (2005) 5183–5195.
- [6] R.H. Lee, B. Kim, I. Choi, H. Kim, H.S. Choi, K. Suh, Y.C. Bae, J.S. Jung, Characterization and expression analysis of mesenchymal stem cells from human bone marrow and adipose tissue, *Cell. Physiol. Biochem.* 14 (2004) 311–324.
- [7] J.G. Toma, M. Akhavan, K.J. Fernandes, F. Barnabe-Heider, A. Sadikot, D.R. Kaplan, F.D. Miller, Isolation of multipotent adult stem cells from the dermis of mammalian skin, *Nat. Cell Biol.* 3 (2001) 778–784.
- [8] C.H. Cui, T. Uyama, K. Miyado, M. Terai, S. Kyo, T. Kiyono, A. Umezawa, Menstrual blood-derived cells confer human dystrophin expression in the murine model of duchenne muscular dystrophy via cell fusion and myogenic transdifferentiation, *Mol. Biol. Cell* 18 (2007) 1586–1594.
- [9] O.K. Lee, T.K. Kuo, W.M. Chen, K.D. Lee, S.L. Hsieh, T.H. Chen, Isolation of multipotent mesenchymal stem cells from umbilical cord blood, *Blood* 103 (2004) 1669–1675.
- [10] M. Terai, T. Uyama, T. Sugiki, X.K. Li, A. Umezawa, T. Kiyono, Immortalization of human fetal cells: the life span of umbilical cord blood-derived cells can be prolonged without manipulating p16INK4a/RB braking pathway, *Mol. Biol. Cell* 16 (2005) 1491–1499.
- [11] X. Zhang, A. Mitsuru, K. Igura, K. Takahashi, S. Ichinose, S. Yamaguchi, T.A. Takahashi, Mesenchymal progenitor cells derived from chorionic villi of human placenta for cartilage tissue engineering, *Biochem. Biophys. Res. Commun.* 340 (2006) 944–952.
- [12] E.H. Allan, P.W. Ho, A. Umezawa, J. Hata, F. Makishima, M.T. Gillespie, T.J. Martin, Differentiation potential of a mouse bone marrow stromal cell line, *J. Cell. Biochem.* 90 (2003) 158–169.
- [13] H. Imabayashi, T. Mori, S. Gojo, T. Kiyono, T. Sugiyama, R. Irie, T. Isogai, J. Hata, Y. Toyama, A. Umezawa, Redifferentiation of dedifferentiated chondrocytes and chondrogenesis of human bone marrow stromal cells via chondrosphere formation with expression profiling by large-scale cDNA analysis, *Exp. Cell Res.* 288 (2003) 35–50.
- [14] S. Makino, K. Fukuda, S. Miyoshi, F. Konishi, H. Kodama, J. Pan, M. Sano, T. Takahashi, S. Hori, H. Abe, J. Hata, A. Umezawa, S. Ogawa, Cardiomyocytes can be generated from marrow stromal cells *in vitro*, *J. Clin. Invest.* 103 (1999) 697–705.
- [15] N. Nishiyama, S. Miyoshi, N.M. Hida, T. Uyama, K. Okamoto, Y. Ikegami, K. Miyado, K. Segawa, M. Terai, M. Sakamoto, S. Ogawa, A. Umezawa, The significant cardiomyogenic potential of human umbilical cord blood-derived mesenchymal stem cells *in vitro*, *Stem Cells* 25 (2007) 2017–2024.
- [16] J. Deng, B.E. Petersen, D.A. Steindler, M.L. Jorgensen, E.D. Laywell, Mesenchymal stem cells spontaneously express neural proteins in culture and are neurogenic after transplantation, *Stem Cells* 24 (2006) 1054–1064.
- [17] H.R. Scholer, G.R. Dressler, R. Balling, H. Rohdewohld, P. Gruss, Oct-4: a germline-specific transcription factor mapping to the mouse t-complex, *EMBO J.* 9 (1990) 2185–2195.
- [18] K. Okamoto, H. Okazawa, A. Okuda, M. Sakai, M. Muramatsu, H. Hamada, A novel octamer binding transcription factor is differentially expressed in mouse embryonic cells, *Cell* 60 (1990) 461–472.
- [19] M.H. Rosner, M.A. Vigano, K. Ozato, P.M. Timmons, F. Poirier, P.W. Rigby, L.M. Staudt, A POU-domain transcription factor in early

- stem cells and germ cells of the mammalian embryo, *Nature* 345 (1990) 686–692.
- [20] M.F. Pera, D. Herszfeld, Differentiation of human pluripotent teratocarcinoma stem cells induced by bone morphogenetic protein-2, *Reprod. Fert. Dev.* 10 (1998) 551–555.
- [21] T. Goto, J. Adjaye, C.H. Rodeck, M. Monk, Identification of genes expressed in human primordial germ cells at the time of entry of the female germ line into meiosis, *Mol. Hum. Reprod.* 5 (1999) 851–860.
- [22] M. Pesce, X. Wang, D.J. Wolgemuth, H. Scholer, Differential expression of the Oct-4 transcription factor during mouse germ cell differentiation, *Mech. Dev.* 71 (1998) 89–98.
- [23] J. Nichols, B. Zevnik, K. Anastassiadis, H. Niwa, D. Klewe-Nebenius, I. Chambers, H. Scholer, A. Smith, Formation of pluripotent stem cells in the mammalian embryo depends on the POU transcription factor Oct4, *Cell* 95 (1998) 379–391.
- [24] H. Niwa, J. Miyazaki, A.G. Smith, Quantitative expression of Oct-3/4 defines differentiation, dedifferentiation or self-renewal of ES cells, *Nat. Genet.* 24 (2000) 372–376.
- [25] B. Abdel-Rahman, M. Fiddler, D. Rappolee, E. Pergament, Expression of transcription regulating genes in human preimplantation embryos, *Hum. Reprod.* 10 (1995) 2787–2792.
- [26] J.L. Chew, Y.H. Loh, W. Zhang, X. Chen, W.L. Tam, L.S. Yeap, P. Li, Y.S. Ang, B. Lim, P. Robson, H.H. Ng, Reciprocal transcriptional regulation of Pou5f1 and Sox2 via the Oct4/Sox2 complex in embryonic stem cells, *Mol. Cell Biol.* 25 (2005) 6031–6046.
- [27] O. Delattre, J. Zucman, B. Plougastel, C. Desmaze, T. Melot, M. Peter, H. Kovar, I. Joubert, P. de Jong, G. Rouleau, A. Aurias, G. Thomas, Gene fusion with an ETS DNA-binding domain caused by chromosome translocation in human tumours, *Nature* 359 (1992) 162–165.
- [28] F. Urano, A. Umezawa, W. Hong, H. Kikuchi, J. Hata, A novel chimera gene between EWS and E1A-F, encoding the adenovirus E1A enhancer-binding protein, in extraosseous Ewing's sarcoma, *Biochem. Biophys. Res. Commun.* 219 (1996) 608–612.
- [29] F. Mitelman, B. Johansson, F. Mertens, The impact of translocations and gene fusions on cancer causation, *Nat. Rev. Cancer* 7 (2007) 233–245.
- [30] M. Kuroda, T. Ishida, M. Takanashi, M. Satoh, R. Machinami, T. Watanabe, Oncogenic transformation and inhibition of adipocytic conversion of preadipocytes by TLS/FUS-CHOP type II chimeric protein, *Am. J. Pathol.* 151 (1997) 735–744.
- [31] S. Yamaguchi, Y. Yamazaki, Y. Ishikawa, N. Kawaguchi, H. Mukai, T. Nakamura, EWSR1 is fused to POU5F1 in a bone tumor with translocation t(6;22)(p21;q12), *Genes Chromosomes Cancer* 43 (2005) 217–222.
- [32] J. Hata, J. Fujimoto, E. Ishii, A. Umezawa, Y. Kokai, Y. Matsubayashi, H. Abe, S. Kusakari, H. Kikuchi, T. Yamada, T. Maruyama, Differentiation of human germ cell tumor cells in vivo and in vitro, *Acta Histochem. Cytochem.* 25 (1992) 563–576.
- [33] E. Schrock, T. Veldman, H. Padilla-Nash, Y. Ning, J. Spurbeck, S. Jalal, L.G. Shaffer, P. Papenhausen, C. Kozma, M.C. Phelan, E. Kjeldsen, S.A. Schonberg, P. O'Brien, L. Biesecker, S. du Manoir, T. Ried, Spectral karyotyping refines cytogenetic diagnostics of constitutional chromosomal abnormalities, *Hum. Genet.* 101 (1997) 255–262.
- [34] M. Sano, A. Umezawa, H. Abe, A. Akatsuka, S. Nonaka, H. Shimizu, M. Fukuma, J. Hata, EAT/mcl-1 expression in the human embryonal carcinoma cells undergoing differentiation or apoptosis, *Exp. Cell Res.* 266 (2001) 114–125.
- [35] S. Gojo, N. Gojo, Y. Takeda, T. Mori, H. Abe, S. Kyo, J. Hata, A. Umezawa, In vivo cardiovascularogenesis by direct injection of isolated adult mesenchymal stem cells, *Exp. Cell Res.* 288 (2003) 51–59.
- [36] T. Sugimoto, A. Umezawa, J. Hata, Neurogenic potential of Ewing's sarcoma cells, *Virchows Arch.* 430 (1997) 41–46.
- [37] Y. Miyagawa, H. Okita, H. Nakajima, Y. Horiuchi, B. Sato, T. Taguchi, M. Toyoda, Y.U. Katagiri, J. Fujimoto, J. Hata, A. Umezawa, N. Kiyokawa, Inducible expression of chimeric EWS/ETS proteins confers Ewing's family tumor-like phenotypes to human mesenchymal progenitor cells, *Mol. Cell Biol.* 28 (2008) 2125–2137.
- [38] B.L. Yen, H.I. Huang, C.C. Chien, H.Y. Jui, B.S. Ko, M. Yao, C.T. Shun, M.L. Yen, M.C. Lee, Y.C. Chen, Isolation of multipotent cells from human term placenta, *Stem Cells* 23 (2005) 3–9.
- [39] E.K. Waller, J. Olweus, F. Lund-Johansen, S. Huang, M. Nguyen, G.R. Guo, L. Terstappen, The "common stem cell" hypothesis reevaluated: human fetal bone marrow contains separate populations of hematopoietic and stromal progenitors, *Blood* 85 (1995) 2422–2435.
- [40] K. Takahashi, K. Tanabe, M. Ohnuki, M. Narita, T. Ichisaka, K. Tomoda, S. Yamanaka, Induction of pluripotent stem cells from adult human fibroblasts by defined factors, *Cell* 131 (2007) 861–872.
- [41] J. Lee, B.K. Rhee, G.Y. Bae, Y.M. Han, J. Kim, Stimulation of Oct-4 activity by Ewing's sarcoma protein, *Stem Cells* 23 (2005) 738–751.
- [42] D. Zhang, A.J. Paley, G. Childs, The transcriptional repressor ZFM1 interacts with and modulates the ability of EWS to activate transcription, *J. Biol. Chem.* 273 (1998) 18086–18091.
- [43] S.L. Palmieri, W. Peter, H. Hess, H.R. Scholer, Oct-4 transcription factor is differentially expressed in the mouse embryo during establishment of the first two extraembryonic cell lineages involved in implantation, *Dev. Biol.* 166 (1994) 259–267.
- [44] T. Barberi, L.M. Willis, N.D. Socci, L. Studer, Derivation of multipotent mesenchymal precursors from human embryonic stem cells, *PLoS Med.* 2 (2005) e161.
- [45] H. Kimura, M. Tada, N. Nakatsuji, T. Tada, Histone code modifications on pluripotential nuclei of reprogrammed somatic cells, *Mol. Cell Biol.* 24 (2004) 5710–5720.
- [46] H.J. Kraft, S. Mosselman, H.A. Smits, P. Hohenstein, E. Piek, Q. Chen, K. Artzt, E.J. van Zoelen, Oct-4 regulates alternative platelet-derived growth factor alpha receptor gene promoter in human embryonal carcinoma cells, *J. Biol. Chem.* 271 (1996) 12873–12878.
- [47] R. Kalluri, E.G. Neilson, Epithelial–mesenchymal transition and its implications for fibrosis, *J. Clin. Invest.* 112 (2003) 1776–1784.
- [48] C. Martinez-Alvarez, M.J. Blanco, R. Perez, M.A. Rabadan, M. Aparicio, E. Resel, T. Martinez, M.A. Nieto, Snail family members and cell survival in physiological and pathological cleft palates, *Dev. Biol.* 265 (2004) 207–218.
- [49] H. Peinado, F. Portillo, A. Cano, Transcriptional regulation of cadherins during development and carcinogenesis, *Int. J. Dev. Biol.* 48 (2004) 365–375.
- [50] E. de Laplanche, K. Gouget, G. Cleris, F. Dragounoff, J. Demont, A. Morales, L. Bezin, C. Godinot, G. Perriere, D. Mouchiroud, H. Simonnet, Physiological oxygenation status is required for fully differentiated phenotype in kidney cortex proximal tubules, *Am. J. Physiol. Renal Physiol.* 291 (2006) F750–F760.
- [51] L.H. Looijenga, H. Stoop, H.P. de Leeuw, C.A. de Gouveia Brazao, A.J. Gillis, K.E. van Roozendaal, E.J. van Zoelen, R.F. Weber, K.P. Wolfenbuttel, H. van Dekken, F. Honecker, C. Bokemeyer, E.J. Perlman, D.T. Schneider, J. Kononen, G. Sauter, J.W. Oosterhuis, POU5F1 (OCT3/4) identifies cells with pluripotent potential in human germ cell tumors, *Cancer Res.* 63 (2003) 2244–2250.